

Bradyrhizobium ivorense sp. nov. as a potential local bioinoculant for *Cajanus cajan* cultures in Côte d'Ivoire

Romain K. Fossou^{1,2}, Joël F. Pothier³, Adolphe Zézé² and Xavier Perret^{1,*}

Abstract

For many smallholder farmers of Sub-Saharan Africa, pigeonpea (*Cajanus cajan*) is an important crop to make ends meet. To ascertain the taxonomic status of pigeonpea isolates of Côte d'Ivoire previously identified as bradyrhizobia, a polyphasic approach was applied to strains CI-1B^T, CI-14A, CI-19D and CI-41S. Phylogeny of 16S ribosomal RNA (rRNA) genes placed these nodule isolates in a separate lineage from current species of the *B. elkanii* super clade. In phylogenetic analyses of single and concatenated partial *dnaK*, *glnII*, *gyrB*, *recA* and *rpoB* sequences, the *C. cajan* isolates again formed a separate lineage, with strain CI-1B^T sharing the highest sequence similarity (95.2%) with *B. tropiciagri* SEMIA 6148^T. Comparative genomic analyses corroborated the novel species status, with 86% ANIb and 89% ANIm as the highest average nucleotide identity (ANI) values with *B. elkanii* USDA 76^T. Although CI-1B^T, CI-14A, CI-19D and CI-41S shared similar phenotypic and metabolic properties, growth of CI-41S was slower in/on various media. Symbiotic efficacy varied significantly between isolates, with CI-1B^T and CI-41S scoring on the *C. cajan* 'Light-Brown' landrace as the most and least proficient bacteria, respectively. Also proficient on *Vigna radiata* (mung bean), *Vigna unguiculata* (cowpea, niébé) and additional *C. cajan* cultivars, CI-1B^T represents a potential bioinoculant adapted to local soil conditions and capable of fostering the growth of diverse legume crops in Côte d'Ivoire. Given the data presented here, we propose the 19 *C. cajan* isolates to belong to a novel species called *Bradyrhizobium ivorense* sp. nov., with CI-1B^T (=CCOS 1862^T=CCMM B1296^T) as a type strain.

Cultivated worldwide as a sole crop or in association with short-maturing cereals and legumes, or with long duration crops like cotton, pigeonpea (*Cajanus cajan* L.) is an important source of proteins for many smallholder farmers of developing countries [1]. In Côte d'Ivoire, diverse *C. cajan* landraces are grown for human consumption and animal feed [2], but also as plants to improve soil fertility in savannahs [3], to reduce soil erosion [4], and to serve as intercrops in upland rice cropping systems [5]. As a legume crop that forms nitrogen-fixing symbioses with soil bacteria collectively known as rhizobia, pigeonpea may overcome the low nitrogen

levels often encountered in tropical and subtropical fields providing proficient rhizobia inhabit those soils. Although pigeonpea was reported to occasionally associate with fast-growing strains of the *Rhizobium* [6, 7] and *Sinorhizobium* (*Ensifer*) [8] genera, most proficient symbionts of *C. cajan* are slow-growing strains that belong to the *Bradyrhizobium* genus [9, 10] with *B. cajan* sp. nov. AMBPC1010^T as the unique type strain that was isolated from a nodule of *C. cajan* during a survey in the Dominican Republic [11].

Author affiliations: ¹Department of Botany and Plant Biology, Microbiology Unit, University of Geneva, Sciences III, 30 quai Ernest-Ansermet, CH-1211 Geneva 4, Switzerland; ²Laboratoire de Biotechnologies Végétale et Microbienne, Unité Mixte de Recherche et d'Innovation en Sciences Agronomiques et Génie Rural, Institut National Polytechnique Felix Houphouët-Boigny, Yamoussoukro, Côte d'Ivoire; ³Environmental Genomics and Systems Biology Research Group, Institute of Natural Resource Sciences, Zurich University of Applied Sciences (ZHAW), Einsiedlerstrasse 31, CH-8820 Wädenswil, Switzerland.

***Correspondence:** Xavier Perret, xavier.perret@unige.ch

Keywords: Africa; symbiosis; nitrogen fixation; legumes; pigeonpea; root nodules.

Abbreviations: ANI, average nucleotide identity; B&D, Broughton and Dilworth nitrogen-free plant growth solution; DDH, DNA-DNA hybridisation; ddH₂O, double distilled water; ML, maximum-likelihood; MLSA, multilocus sequence analysis; RMM, Rhizobium minimal medium; RMS, RMM medium supplemented with succinate.

All sequences determined for *Bradyrhizobium ivorense* sp. nov. isolates described in this study were deposited in GenBank/EMBL/DBJ under the following accessions: *dnaK* of strain CI-1B^T (MK376326), CI-14A (MK376327), CI-19D (MK376328), CI-41S (MK376329); *glnII* of strain CI-1B^T (MH756157), CI-14A (MH756158), CI-19D (MH756159), CI-41S (MH756160); *gyrB* of strain CI-1B^T (MH756161), CI-14A (MH756162), CI-19D (MH756163), CI-41S (MH756164); *recA* of strain CI-1B^T (MK376330), CI-14A (MK376331), CI-19D (MK376332), CI-41S (MK376333); *rpoB* of strain CI-1B^T (KX388393), CI-14A (MK376334), CI-19D (MK376335), CI-41S (MK376336). Genome sequences for CI-1B^T and CI-41S strains can be accessed via GenBank Assembly accessions GCA_900696085 and GCA_900696075, respectively.

Eight supplementary figures and eight supplementary tables are available with the online version of this article.

003931 © 2019 The Authors



Initially proposed by Jordan as a separate taxon for slow-growing root nodule bacteria of legumes [12], the genus *Bradyrhizobium* now encompasses more than 50 proposed species [13]. Phylogenetic analyses based upon sequences of the 16S ribosomal RNA (rRNA) and several core protein genes, later separated bradyrhizobia species into two main lineages: the *B. japonicum* and *B. elkanii* super clades [14]. More recent phylogenetic analyses on larger sets of isolates and gene sequences showed bradyrhizobia strains clustered into more than two discreet subgroups, however [13, 15]. Nevertheless, with more than 30 species the *B. japonicum* supergroup includes plant associated bacteria as diverse as *B. arachidis* CCBAU 051107^T that was isolated from root nodules of *Arachis hypogaea* in Hebei, China [16]; *B. betae* LMG 21987^T from a tumour-like outgrowth of sugar beet (*Beta vulgaris*) grown in northern Spain [17]; *B. canariense* BTA-1^T that nodulated genistoid legumes from the Canary Islands [18]; *B. diazoefficiens* (previously *japonicum*) USDA 110^T that was isolated from a soybean nodule in Florida (US Department of Agriculture, Beltsville, MD); *B. iriomotense* strain EK05^T which infected a root-outgrowth of an *Entada koshunensis* legume in the Okinawa island in Japan [19]; *B. japonicum* USDA 6^T that was found in a soybean nodule collected in Japan and entered a strain collection as early as 1929 [20]; the extra-slow growing *B. liaoningense* USDA 3622^T (ESG 2281^T) found inside a soybean nodule collected in the Heilongjiang Province of PR China [21]; *B. ottawaense* OO99^T isolated from a soybean field near Ottawa, Canada [22] as well as the *B. cajani* AMBPC1010^T described above [11]. Together, these nine type strains of the *B. japonicum* lineage already illustrate the diversity, ubiquitous geographic distribution and relative plant promiscuity that characterise many of the bradyrhizobia strains [13].

Yet, as recently noted by Grönemeyer and Reinhold-Hurek [23], our knowledge on the diversity and biogeography of bradyrhizobia species relies primarily on data collected in the Americas, Asia and Europe. For examples, type strains of the *B. elkanii* supergroup include *B. icense* LMTR 13^T isolated from *Phaseolus lunatus* in Peru [24]; *B. macuxiense* UFLA03-321^T found inside a nodule of *Centrolobium parensis* in Amazonia [25] and *B. retamae* Ro19^T identified as a symbiont of *Retama monosperma* in the Mediterranean basin [26]. A number of recent surveys identified bradyrhizobia in sub-Saharan countries, however, including in Angola and Namibia [27], Ethiopia [14], Kenya [28] and Senegal [29]. In addition, a sampling of six fields in three geographically distant regions of Côte d'Ivoire has led to the molecular characterisation of >80 pigeonpea isolates by matrix-assisted laser desorption/ionization (MALDI) time of flight (TOF) mass spectrometry (MS) and DNA sequencing [30]. That data indicated that 63 of the 85 nodule isolates (74%) were bradyrhizobia, only one of which (strain CI-41A) belonged to the *B. japonicum* super clade. Hierarchical cluster analysis of mass spectra separated the remaining 62 nodule isolates into a group of 43 strains close to *B. elkanii* USDA 76^T (cluster I strains) and a second group of 19 bradyrhizobia (cluster II), whose taxonomic status was unclear. Phylogenetic analyses reported herein show

the cluster II strains to belong to a separate lineage of the *B. elkanii* super clade, with levels of similarity for partial *dnaK*, *glnII*, *gyrB*, *recA* and *rpoB* sequences and genomic average nucleotide identity (ANI) values supporting the designation of *Bradyrhizobium ivorense* sp. nov. as a novel species with CI-1B^T being proposed as the type strain.

PHYLOGENETIC CHARACTERIZATION

Although still recognized as universal genetic markers for classifying bacterial isolates, 16S rRNA sequences were occasionally found to be too conserved for accurately delineating bradyrhizobia species [24, 31]. By contrast multilocus sequence analysis (MLSA) of concatenated partial sequences for conserved protein-coding genes has been shown to provide reliable phylogenies, to reflect overall genome similarities and to match DNA-DNA hybridization (DDH) values [32]. MLSA has been repeatedly used for resolving bradyrhizobia lineages and has become one of the hallmark criteria for delimiting novel species (e.g [33, 34].) Similarly, DDH, that was long considered as another 'gold standard' for delimiting bacterial species, has been superseded by the more informative pairwise comparisons of genome sequences [35, 36]. Accordingly, a polyphasic approach was applied to determine the taxonomic status of the 19 pigeonpea isolates of Côte d'Ivoire grouped in cluster II. Isolates CI-1B^T, CI-14A, CI-19D and CI-41S were selected as representative strains because they originated from different fields and regions of Côte d'Ivoire (Table S1, available in the online version of this article) and possessed protein mass spectra that reflected the genetic diversity existing within cluster II isolates [30]. For long term preservation, 30% glycerol stocks were kept at -60 °C and bacteria were routinely grown in/on *Rhizobium* minimal medium (RMM) supplemented with 12 mM succinate (RMS) [37], or in/on RMM containing alternative carbon sources when specific metabolic analyses were needed.

For MLSA studies, the *dnaK*, *glnII*, *gyrB*, *recA* and *rpoB* marker genes were amplified using procedures described in Fossou et al. [30] and primers specifically designed for bradyrhizobia sequences (Table S2). Marker genes were sequenced on both strands using Sanger sequencing. The resulting sequences were assembled and manually curated for primers and ambiguities before being archived in GenBank, with their respective accession numbers listed in Table S2. As preliminary analyses showed the pigeonpea isolates to share identical 16S rDNA sequences and to belong to the *B. elkanii* super clade [30], subsequent phylogenetic analyses included all 21 types strains currently described for this lineage. An additional eight type strains representative of the *B. japonicum* super clade as well as the unrelated *B. oligotrophicum* LMG 10732^T strain were also included in phylogenies [13]. Together with the associated accession numbers that characterise them, the bradyrhizobia type strains of the *B. japonicum* and *B. elkanii* super clades are listed in Tables S3a and S3b, respectively. Except for type strains of the *B. erythrophlei*, *B. ferriligni*, *B. namibiense* and *B. ripae* species for which no genome data was accessible at the time of writing, all other sequence accessions

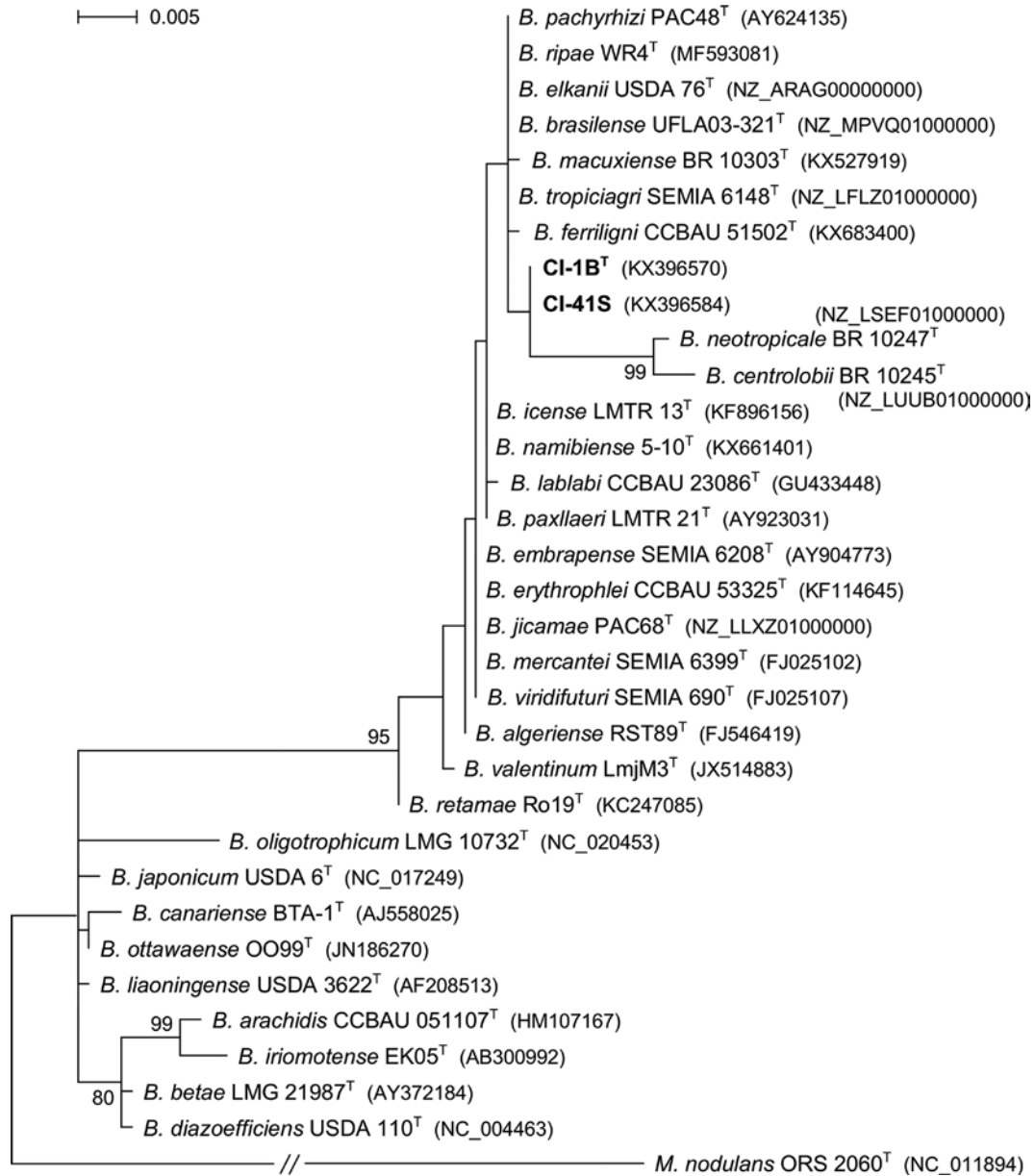


Fig. 1. Maximum-likelihood (ML) unrooted phylogeny of 16S rRNA gene sequences of type strains of the *Bradyrhizobium* genus and of *B. ivorensis* sp. nov. CI-1B^T and CI-41S. Sequences were aligned with MAFFT version 7 using the Q-INS-i method. Analysis used the T92 +G+I model, a total of 1182 positions, 1000 pseudoreplicates with bootstrap values >70% shown at branch nodes. Sequences for the 21 members of the *B. elkanii* super clade and *B. oligotrophicum* LMG 10732^T were 1179 bp long. Except for *B. iriomotense* (1178 bp), sequences for the *B. japonicum* super clade type strains were 1177 bp long. To improve resolution of ML tree, the branch for the *M. nodulans* strain ORS 2060^T outgroup was truncated. Accession numbers or source for 16S rRNA gene sequences are indicated within parentheses next to the species name, with strains of the novel species marked in bold. Bar represents the expected number of substitutions per site.

were manually curated using as reference the corresponding genomic data, and inaccuracies were highlighted in Table S3b. In the case of *B. ferriligni* type strain CCBAU 51502^T, the 16S rRNA gene sequence archived under GenBank accession KX683400 (deposited by Li Y. in 2016) was used instead of the KJ818096 sequence (deposited by Yao and Sui in 2014), which diverged too much from other bradyrhizobia sequences to be considered as reliable. DNA sequences were aligned with

MUSCLE as implemented in MEGA software version 7 [38], and partial housekeeping gene sequences concatenated with Seaview ver. 4 [39]. Phylogenies were inferred with MEGA 7, with evolutionary trees reconstructed using the maximum likelihood (ML) method [40], a statistical support of 1000 bootstrap replicates and sequences of *Methylobacterium nodulans* strain ORS 2060^T [41] selected as outgroups. Best-fit nucleotide substitution model was selected according

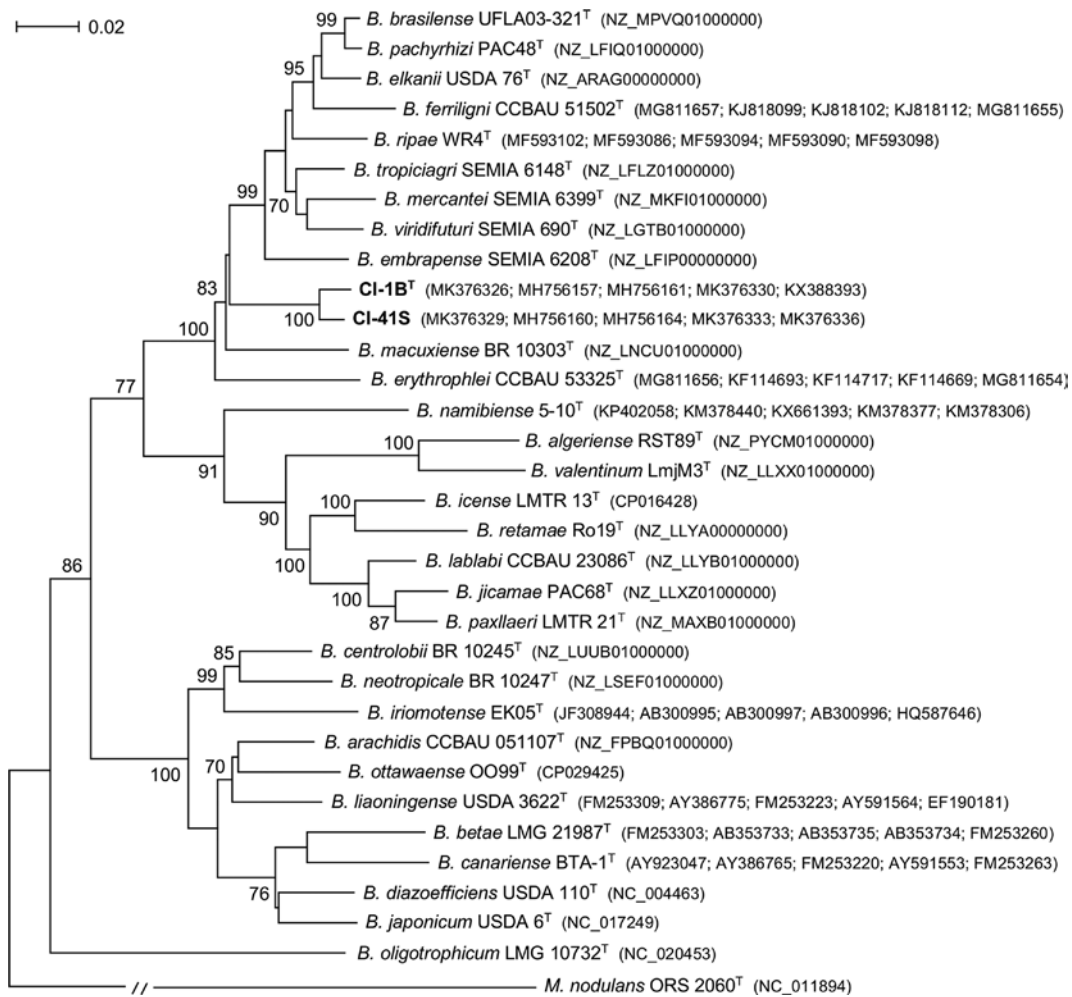


Fig. 2. Maximum-likelihood (ML) unrooted phylogram inferred from concatenated partial *dnaK* (279 bp), *glnII* (540 bp), *gyrB* (588 bp), *recA* (439 bp) and *rpoB* (714 bp) gene sequences of type strains of the *Bradyrhizobium* genus and of *B. ivorense* sp. nov. CI-1B^T and CI-41S. The GTR+G+I model was used and included as parameters a total of 2566 positions and 1000 pseudoreplicates, with only bootstrap support values >70% shown at branch nodes. To improve resolution of the tree, the branch for the *M. nodulans* strain ORS 2060^T outgroup was truncated. Accession numbers or source for sequences are indicated within parentheses next to the species name. Bar represents the expected number of substitutions per site.

to the Bayesian information criterion [42], and similarity levels (uncorrected genetic distances) between concatenated sequences of selected *Bradyrhizobium* species calculated as in Rashid *et al.* [43] and reported in Table S4.

Because pigeonpea isolates CI-1B^T, CI-14A, CI-19D and CI-41S share identical 16S rRNA gene sequences [30], only CI-1B^T and CI-41S are displayed in the ML phylogenetic trees for that marker. As expected, in the phylogeny based upon 1182 positions of nearly complete 16S rRNA gene sequences that are shown in Figures 1 and S1, the taxonomic position of many of the 21 species of the *B. elkanii* supergroup (e.g. *B. elkanii* USDA 76^T, *B. pachyrhizi* PAC48^T, *B. ripae* WR4^T and *B. tropiciagri* SEMIA 6148^T) remained unresolved. Yet, strains CI-1B^T and CI-41S always formed a distinct branch rooted in the *B. elkanii* clade of 16S rRNA gene trees, whether a subset of eight representative or 34 species of the *B. japonicum*

supergroup were included in the analyses (see Figs 1 and S1, respectively). Phylogenetic relationships between the *C. cajan* isolates and bradyrhizobia type strains was better resolved by applying MLSA using the following partial *dnaK* (MK376326 to MK376329), *glnII* (MH756157 to MH756160), *gyrB* (MH756161 to MH756164), *recA* (MK376330 to MK376333) and *rpoB* (MK376334 to MK376336) gene sequences for the *C. cajan* isolates (see also Table S2). In order to include the same set of 30 type strains used for the 16S rRNA gene phylogeny shown in Fig. 1, individual alignment lengths were trimmed to 279 (*dnaK*), 540 (*glnII*), 588 (*gyrB*), 439 (*recA*) and 714 (*rpoB*) nucleotides. As preliminary phylogenetic analyses confirmed that trees for each of the five selected markers were largely congruent (see Fig. S2–S6), individual sequences were combined into a dataset of 2560 bp long concatenated sequences which phylogeny showed CI-1B^T

Table 1. Average nucleotide identity (ANI) values between *Bradyrhizobium ivorense* sp. nov. CI-1B^T, CI-41S and type strains of the *B. elkanii* super clade with available genome data

Strains	CI-1B ^T	
	ANiB (%)	ANIm (%)
<i>B. ivorense</i> sp. nov. CI-41S	96.6	97.5
<i>B. elkanii</i> USDA 76 ^T	86.0	89.0
<i>B. pachyrhizi</i> PAC48 ^T	85.4	88.6
<i>B. macuxiense</i> UFLA03-321 ^T	85.3	88.7
<i>B. mercantei</i> SEMIA 6399 ^T	85.2	88.6
<i>B. tropiciagri</i> SEMIA 6148 ^T	85.2	88.4
<i>B. embrapense</i> SEMIA 6208 ^T	85.0	88.3
<i>B. viridifuturi</i> SEMIA 690 ^T	85.0	88.3
<i>B. brasiliense</i> BR 10303 ^T	84.1	87.9
<i>B. lablabi</i> CCBAU 23086 ^T	79.7	85.2
<i>B. jicamae</i> PAC68 ^T	79.4	85.4
<i>B. paxllaeri</i> LMTR 21 ^T	79.4	85.4
<i>B. algeriense</i> RST89 ^T	79.2	85.2
<i>B. icense</i> LMTR 13 ^T	78.9	85.3
<i>B. retamae</i> Ro19 ^T	78.9	85.2
<i>B. valentinum</i> LmjM3 ^T	78.9	85.2

and CI-41S to form a separate, highly supported lineage in a basal position of the *B. elkanii* super clade (Fig. 2). While concatenated sequences of CI-1B^T and CI-41S shared 98.4% similarity, the highest levels of sequence similarity between CI-1B^T and bradyrhizobia type strains was with *B. tropiciagri* SEMIA 6148^T (95.2%), followed by *B. elkanii* USDA 76^T, *B. pachyrhizi* PAC48^T and *B. ripae* WR4^T (95.1%) (see Table S4). Surprisingly, in this study, several type strains shared sequence similarities above the 97% threshold recently proposed to separate bradyrhizobia species, when a similar set of marker genes (*atpD*, *dnaK*, *glnII*, *gyrB*, *recA*) was used [24]. For example, concatenated sequences of *B. pachyrhizi* PAC48^T and *B. brasiliense* UFLA03-321^T shared as much as 99.1% similarity, while *B. elkanii* USDA 76^T and *B. pachyrhizi* PAC48^T genes were 97.8% similar (Table S4), therefore the use of 97% sequence similarity threshold for delimiting potential *Bradyrhizobium* species requires further investigation. That *B. ivorense* isolates form a separate lineage within the *B. elkanii* clade was further confirmed by a phylogenetic analysis of concatenated partial *glnII* (522 bp) and *recA* (411 bp) gene sequences of CI-1B^T, CI-41S and 57 *Bradyrhizobium* type strains (see Fig. S7).

GENOMIC CHARACTERIZATION

To further characterize the *C. cajan* isolates, draft genomes were obtained for CI-1B^T and CI-41S using paired-end sequencing (2×300 bp) with an Illumina MiSeq instrument at the Zürich University of Applied Sciences (ZHAW). Once isolated via a NucleoSpin tissue kit (Macherey-Nagel, Düren, Germany),

Table 2. Differential characteristics of *Bradyrhizobium ivorense* sp. nov. isolates, using as reference strain *B. elkanii* USDA 76^T that was grown in the same conditions. For comparison, corresponding phenotypes of *B. pachyrhizi* PAC48^T and *B. tropiciagri* SEMIA 6148^T were taken from Ramírez-Bahena et al. (2009) [52] and Delamuta et al. (2015) [53], respectively. Bacterial response was qualified as: +, positive; ±, weak or variable; -, negative; or ND, not determined

Differential characteristics	Strains						
	CI-1B ^T	CI-14A	CI-19D	CI-41S	USDA 76 ^T	PAC48 ^T	SEMIA 6148 ^T
Growth at 35 °C	-	-	±	±	+	+	+
Aesculin hydrolysis	±	-	-	ND	-	±	±
Reduction of nitrate to nitrite	-	-	-	-	+	+	ND
Assimilation as carbon source:							
Arabinose	+	±	+	ND	±	+	+
Glucose	+	±	+	±	±	+	-
Maltose	+	+	+	±	±	±	-
<i>N</i> -acetylglucosamine	+	+	+	ND	±	-	-
Resistant to (µg per disc):							
Ampicillin (100)	+	+	±	-	-	±	ND
Kanamycin (100)	+	+	+	+	-	-	ND
Growth in YM with 0.5% NaCl	+	+	-	+	+	+	+
0.75% NaCl	-	-	-	-	+	+	+

Table 3. Profiles of cellular fatty acids detected in *Bradyrhizobium ivorense* sp. nov. isolates CI-1B^T and CI-41S and in *B. elkanii* USDA 76^T as a reference strain. Reported values correspond to percentages of the total amount of fatty acid compounds found in each strain. Not detected, ND

Fatty acid compound detected	Strain		
	CI-1B ^T	CI-41S	USDA 76 ^T
C _{12:1} 3-OH	0.42	ND	ND
C _{14:0}	ND	0.50	ND
C _{16:0}	9.68	12.31	7.23
C _{16:1} ω5cis	0.31	ND	0.16
C _{16:1} ω7cis, C _{16:1} ω6cis	1.83	1.18	0.55
C _{17:0}	ND	ND	0.36
C _{17:0} cyclo	ND	ND	1.13
C _{17:1} ω8cis	ND	ND	0.31
C _{18:0}	0.40	0.58	0.57
C _{18:1} ω5cis	0.47	0.35	0.68
C _{18:1} ω7cis	86.03	81.30	67.88
C _{19:0} cyclo ω8cis	0.86	3.78	21.01
C _{20:1} ω7cis	ND	ND	0.11

genomic DNAs of CI-1B^T and CI-41S were fragmented with a Covaris E220 ultrasonicator, aiming for an average target size of 550 bp. Preparation of sequencing libraries followed the Illumina NeoPrep library system protocol. A total of 5090206 and 1570172 reads were obtained that provided a sequencing coverage of 115- and 36-folds for CI-1B^T and CI-41S, respectively. *De novo* sequence assemblies were obtained with MIRA version 4.0 [44] using standard settings in accurate mode. This was followed by contig reassembly using SeqMan Pro from the Lasergene genomics package version 12.1.0 (DNASTar, Madison, WI) with Pro assembler parameters and read mapping using SeqMan NGen with standard settings to check for mapping inconsistencies. Sequence contigs were ordered using Mauve 20150226 version 10 [45] and the genome of *B. elkanii* USDA 76^T as reference. Automatic genome annotation was performed using the Prokka software tool version 1.12 [46]. The main characteristics of the CI-1B^T and CI-41S genomes are reported in Table S5, with individual sequence contigs archived under the GenBank Nucleotide accessions CAADFC020000001 to CAADFC020000044 for strain CI-1B^T and CAADFB020000001 to CAADFB020000059 for strain CI-41S. ANI values between *B. ivorense* sp. nov. CI-1B^T and CI-41S, and the type strains *B. algeriense* RST89^T (PYCM01000000), *B. brasiliense* BR 10303^T (MPVQ01000000), *B. elkanii* USDA 76^T (ARAG00000000), *B. embrapense* SEMIA 6208^T (LFIP00000000), *B. icense* LMTR 13^T (CP016428), *B. jicamae* PAC68^T (LLXZ01000000), *B. lablabi* CCBAU 23086^T (LLYB01000000), *B. macuxiense* UFLA03-321^T (LNCU01000000), *B. mercantei* SEMIA 6399 (MKFI01000000), *B. pachyrhizi* PAC 48^T (LFIQ01000000),

B. paxllaeri LMTR 21^T (MAXB01000000), *B. retamae* Ro19^T (LLYA00000000), *B. tropiciagri* SEMIA 6148^T (LFLZ01000000), *B. valentinum* LmjM3^T (LLXX01000000) and *B. viridifuturi* SEMIA 690^T (LGTB01000000) were calculated with JSpeciesWS [47] using BLAST (ANIb) and Mummer (ANIm) for sequence alignments [48]. Calculations showed that CI-1B^T and closely related bradyrhizobia type strains shared as highest ANIb and ANIm, values of 86 and 89%, respectively (Table 1). Since both calculated ANIb and ANIm scores are well below the 95–96% threshold proposed for delineating species [48], genomic data also supported the proposal that cluster II *C. cajan* isolates belong to a novel *Bradyrhizobium* species.

PHENOTYPIC CHARACTERIZATION

Metabolic properties of *C. cajan* isolates were characterised using a number of assays and *B. elkanii* USDA 76^T as the reference type strain. At first, API 20 NE strips (BioMérieux SA, Marcy-l'Étoile, France) were used, with slower growth of bradyrhizobia implying modifications to the manufacturer's protocol as described below. Cells were precultured at 27 °C in RMS [37] to an OD₆₀₀ of 0.6 then washed in sterile 0.5% NaCl solution. Slots for enzymatic reactions were inoculated with 10⁸ cells resuspended in saline solution, whereas ca. 10⁷ cells in RMM agar were inoculated onto the various carbon sources included in the assay. Duplicated API galleries were incubated at 27 °C, in a sterile and sealed container with a moist atmosphere, with reactions assessed every second day for at least 2 weeks. When needed, sterile ddH₂O was added to compensate for evaporation. Utilization of several carbon sources was validated by additional *in vitro* assays carried out in RMM liquid cultures of 5 ml supplemented with 10 mM succinate or malate, or 20 mM galactose, glucose, fructose, maltose, mannose, pyruvate or sucrose. Cultures were inoculated with 10⁷ fresh cells, in duplicate for each strain, and incubated at 27 °C with shaking, with growth monitored every third day and considered as positive if OD₆₀₀ > 0.2 after 10 days. For growth at different NaCl concentrations, OD₆₀₀ was measured every second day for a week. Catalase activity was determined by rubbing colonies onto a glass slide in presence of 3% H₂O₂ and checking for presence of bubbles. Oxidase activity was detected by rubbing colonies on a Whatman paper soaked with 0.1% *N,N*-dimethyl-1,4-phenylenediamine oxalate solution. Sensitivity to antibiotics was determined with large (Ø145 mm) RMS agar plates pre-inoculated with 10⁸ cells from early log phase (0.2 < OD₆₀₀ < 0.4) RMS cultures onto which antibiotic discs were placed at equidistance. Discs contained the following amounts of antibiotics: ampicillin 100 µg, chloramphenicol 500 µg, erythromycin 50 µg, gentamycin 50 µg, kanamycin 100 µg, penicillin 10 µg, streptomycin 250 µg or tetracycline 50 µg. For each strain, tests were duplicated with plates incubated at 27 °C for a maximum of 10 days, with cells considered as sensitive to the antibiotic if a growth halo of Ø > 2 mm was observed from the disc edge [49]. Differential growth and metabolic properties of *C. cajan* isolates and of USDA 76^T strain are reported in Table 2, with all phenotypic characteristics listed in Table S6.

Table 4. Symbiotic efficacy of selected *Bradyrhizobium ivorense* isolates on the *Cajanus cajan* 'Light Brown' landrace. Strain proficiency is reported as the mean nodule number (mNN), nodule fresh weight (mNFW) and shoot dry weight (mSDW) per plant, with standard deviations shown in parentheses. SDW values marked with an asterisk were found to be statistically different from the corresponding values measured for CI-1B^T at the level $\alpha=5\%$

Strain	Test	Plants	mNN	mNFW (mg)	mSDW (mg)
No inoculum	1	6	0.0	0.0	73.7 (± 7.9)*
	2	5	0.0	0.0	83.4 (± 33.2)*
<i>Bradyrhizobium elkanii</i> USDA 76 ^T	1	8	32.0 (± 5.8)	898.0 (± 227.5)	2176.1 (± 471.7)
	2	7	46.0 (± 9.4)	1160.6 (± 183.0)	2700.4 (± 342.7)
CI-1B ^T	1	8	75.1 (± 25.3)	1581.1 (± 477.2)	2655.0 (± 777.7)
	2	8	75.9 (± 12.5)	1624.1 (± 213.1)	3041.6 (± 483.7)
CI-4A2	1	8	59.1 (± 18.6)	1050.5 (± 377.8)	1876.3 (± 449.8)*
CI-4A3	2	8	80.4 (± 19.6)	1140.3 (± 148.9)	2386.8 (± 412.3)*
CI-4C	1	8	75.6 (± 17.0)	1534.4 (± 357.6)	2718.3 (± 600.2)
CI-4D	2	8	100.0 (± 35.2)	1208.1 (± 286.1)	2230.3 (± 404.5)*
CI-14A	1	8	58.6 (± 11.4)	925.3 (± 210.2)	2112.6 (± 527.5)
CI-15A	2	8	35.9 (± 8.0)	1184.4 (± 140.8)	3027.1 (± 574.0)
CI-18C	1	7	46.9 (± 17.0)	943.0 (± 292.2)	1833.7 (± 482.9)*
CI-19D	1	8	36.5 (± 7.3)	896.1 (± 133.9)	1933.3 (± 337.3)*
CI-33F	2	8	62.4 (± 18.7)	1033.8 (± 245.2)	1637.3 (± 355.5)*
CI-35B	1	8	75.4 (± 18.8)	910.5 (± 203.5)	1765.9 (± 426.1)*
CI-41S	1	8	39.4 (± 7.7)	492.5 (± 113.3)	691.0 (± 156.3)*
	2	8	36.5 (± 7.3)	896.1 (± 133.9)	1155.1 (± 403.8)*

The composition in cellular fatty acids of strains CI-1B^T and CI-41S was analysed at the Culture Collection of Switzerland (CCOS) in Wädenswil (Switzerland) using standard procedures and gas-chromatography-based analyses. As a reference control, the fatty acid composition of the *B. elkanii* USDA 76^T type strain was determined in parallel. The fatty acid profile obtained for USDA 76^T matched well the mean fatty acid concentrations determined for group I *B. elkanii* strains by Tighe and co-workers [50], with predominant fatty acids being of the C_{18:1} $\omega 7cis$ [67.88% vs. 67.05 (± 5.04)% in Tighe *et al.* 2000], C_{19:0} cyclo $\omega 8cis$ [21.01% vs. 19.99 (± 3.47)%] and C_{16:0} [7.23% vs. 10.49 (± 2.35)%] forms. Although CI-1B^T and CI-41S strains contained lower concentrations of C_{19:0} cyclo $\omega 8cis$ (0.86% in CI-1B^T and 3.78% in CI-41S), the most abundant fatty acids remained of the C_{18:1} $\omega 7cis$ and (86.03 and 81.3%, respectively) and C_{16:0} (9.68 and 12.31%, respectively) types. Other differences between the CI-1B^T, CI-41S and USDA 76^T strains are the absence in the pigeonpea isolates of the C_{17:0} cyclo compound found in USDA 76^T at 1.13%, and the presence in CI-41S of C_{14:0} that was not detected in the other two strains. The respective concentrations of cellular fatty acids reliably detected in extracts are reported in Table 3.

To examine the symbiotic properties of *B. ivorense* sp. nov., strains were inoculated onto *C. cajan* cv. 'Light Brown' (see [30]), *Glycine max* cv. Davis, *Macroptilium atropurpureum*

cv. Siratro, *Leucaena leucocephala*, *Tephrosia vogelii*, *Vigna radiata* cv. King (mung bean), and *V. unguiculata* cv. Red Caloona (cowpea). Nodulation assays were carried out in autoclaved Magenta jars containing vermiculite and nitrogen free B&D as a plant growth solution [51], using two plants per pot, an inoculum of 2×10^8 bacteria per seedling and controlled growth conditions of 12 h light phase at 10000 Lux and night/day temperatures of 20/27 °C, respectively. Depending on the legume species, plants were grown for 35 to 98 days post inoculation (dpi) with as many as 12 different *C. cajan* isolates being tested for assessing the diversity of symbiotic responses, for example in function of the geographic distribution of strains. As shown in Table 4, on *C. cajan* cv. 'Light Brown' symbiotic efficacy of *B. ivorense* sp. nov. isolates varied considerably, with CI-1B^T, CI-4C and CI-15A being the most proficient strains when shoot dry weight (SDW) was selected as criterion. When inoculated onto other legume species, *C. cajan* isolates formed nitrogen fixing nodules on cowpea, mungbean and siratro, pseudonodules on *L. leucocephala* and few sporadic pink nodules on soybean cv. Davis (see Table S7). Interestingly, on all plant species tested, CI-41S was always the least proficient bacterium, except on *T. vogelii* on which CI-41S was nearly as proficient as CI-1B^T and clearly more effective than the promiscuous *Sinorhizobium fredii* strain NGR234. Together, these nodulation assays confirmed

that strain CI-1B^T was highly proficient on several legume crops cultivated by smallholder farmers in West Africa, including cowpea (also known locally as 'niébé'), mungbean and pigeonpea. In respect to nitrogen fixation genes, CI-1B^T, CI-14A, CI-19D and CI-41S share nearly identical *nifH* genes [30], with corresponding loci of *B. elkanii* USDA 76^T and *B. ferriligni* CCBAU 51502^T strains being the closest in the *nifH* phylogeny shown in Fig. S8.

DESCRIPTION OF *BRADYRHIZOBIUM IVORENSE* SP. NOV.

Bradyrhizobium ivorense (i.vor.en'se. N.L. neut. adj. *ivorense* referring to Côte d'Ivoire, the country where isolates of this species were collected from *C. cajan* nodules).

Cells are Gram-stain-negative, aerobic, 0.6–0.7 µm wide by 1.1–3.4 µm long rods of size similar to other members of the genus. Generation time of the proposed *B. ivorense* sp. nov. CI-1B^T strain was estimated at 14 h (±3 h) when cells were grown in RMS liquid cultures and at 27 °C. On RMS agar, colonies are whitish, convex, circular, with 2 to 3 mm diameter after 10 days incubation at 27 °C. Optimal growth was observed at neutral pH, at temperatures comprised between 25 to 30 °C, and at NaCl concentrations <0.5%. Although some growth still occurred at 20 and 35 °C, plates incubated at 40 °C exhibited no growth. Strains CI-1B^T, CI-14A and CI-19D did not show significant inhibition zones when in presence of all antibiotics tested, at least when challenged with discs containing the following amounts: ampicillin 100 µg, chloramphenicol 500 µg, erythromycin 50 µg, gentamycin 50 µg, kanamycin 100 µg, penicillin 10 µg, streptomycin 250 µg or tetracycline 50 µg. Strain CI-41S was found to be sensitive to ampicillin 100 µg but grew in presence of other antibiotic discs. Strains CI-1B^T, CI-14A and CI-19D were all positive for oxidase, arginine dihydrolase and urease reactions, while only CI-1B^T responded weakly to aesculin hydrolysis. These same three strains were all negative for catalase, D-glucose fermentation, gelatin hydrolysis, indole production, nitrate reduction and para-nitrophenyl-β-D-galactopyranosidase reactions. Assimilation tests were positive for adipic acid, D-glucose, maltose, D-mannitol, D-mannose, L-arabinose, N-acetyl-glucosamine and potassium gluconate; weak for malic acid, trisodium citrate, phenylacetic acid; and negative for capric acid. In addition, CI-1B^T and CI-41S were found to assimilate fructose, galactose, malate and pyruvic acid; but apparently could not use sucrose as sole carbon source. Effective nodules were formed on *C. cajan*, *M. atropurpureum*, *V. radiata*, *V. unguiculata* and *T. vogelii* but not on *G. max* and *L. leucocephala*.

The type strain, CI-1B^T (=CCOS 1862^T=CCMM B1296^T) was isolated from a root nodule of a *C. cajan* plant growing in Kossou-Bouafla, Côte d'Ivoire. The draft genome of the type strain is characterized by a size of 9.4 Mbp and a G+C content of 64.2 mol%. The GenBank accession number of the 16S rRNA gene sequence of strain CI-1B is KX396570, and its draft genome sequence accession number is GCA_900696085.

Funding information

Financial support for this work was provided by the University of Geneva and the Swiss National Science Foundation (grants 31 003A-146548 and 31 003A-173191).

Acknowledgements

The 19 *B. ivorense* sp. nov. strains described in this work were all isolated from nodules of pigeonpea collected in fields of Côte d'Ivoire (see [30]). Sampling of the *C. cajan* nodules in fields of Côte d'Ivoire was supported by a research collaboration fellowship attributed by the Centre Suisse de Recherche Scientifique (CSRS) of Abidjan to Adolphe Zézé (AZ) and Xavier Perret (XP), thanks to a donation of the United Nations Development Program. Transfer of *C. cajan* nodules to the University of Geneva and the subsequent genotyping of the rhizobia isolated from these nodules, were subject to conditions described in a Material Transfer Agreement that was signed by AZ and XP on July 12, 2012.

Conflicts of interest

The authors declare that there are no conflicts of interest.

References

1. Varshney RK, Penmetsa RV, Dutta S, Kulwal PL, Saxena RK et al. Pigeonpea genomics initiative (PGI): an international effort to improve crop productivity of pigeonpea (*Cajanus cajan* L.). *Mol Breed* 2010;26:393–408.
2. Fossou RK, Kouassi NKI, Kouadio GCZ, Zako S, Zézé A. Diversité de rhizobia dans un Champ cultivé de pois d'Angole (*Cajanus cajan* L.) Yamoussoukro (centre de la Côte d'Ivoire). *Agronomie Africaine* 2012;24:29–38.
3. Koné AW, Edoukou EF, Tondoh JE, Gonnety JT, Angui PKT et al. Comparative study of earthworm communities, microbial biomass, and plant nutrient availability under 1-year *Cajanus cajan* (L.) Millsp and *Lablab purpureus* (L.) Sweet cultivations versus natural regrowths in a guinea savanna zone. *Biol Fertil Soils* 2012;48:337–347.
4. Charpentier H, Doumbia S, Coulibaly Z, Zana O. Fixation de l'agriculture au Nord et au centre de la Côte d'Ivoire: quels nouveaux systèmes de culture? *Agri Dév* 1999;21:41–70.
5. Akanvou R, Kropff MJ, Bastiaans L, Becker M. Evaluating the use of two contrasting legume species as relay intercrop in upland rice cropping systems. *Field Crops Res* 2002;74:23–36.
6. Degefu T, Wolde-meskel E, Frostegård Åsa. Phylogenetic diversity of *Rhizobium* strains nodulating diverse legume species growing in Ethiopia. *Syst Appl Microbiol* 2013;36:272–280.
7. Wolde-Meskel E, Terefeork Z, Frostegård A, Lindström K. Genetic diversity and phylogeny of rhizobia isolated from agroforestry legume species in southern Ethiopia. *Int J Syst Evol Microbiol* 2005;55:1439–1452.
8. Stępkowski T, Czaplinska M, Miedzinska K, Moulin L. The variable part of the *dnaK* gene as an alternative marker for phylogenetic studies of rhizobia and related alpha *Proteobacteria*. *Syst Appl Microbiol* 2003;26:483–494.
9. Araújo J, Díaz-Alcántara C-A, Velázquez E, Urbano B, González-Andrés F. *Bradyrhizobium yuanmingense* related strains form nitrogen-fixing symbiosis with *Cajanus cajan* L. in Dominican Republic and are efficient biofertilizers to replace N fertilization. *Sci Hortic* 2015;192:421–428.
10. Ramsuhag A, Umaharan P, Donawa A. Partial 16S rRNA gene sequence diversity and numerical taxonomy of slow growing pigeonpea (*Cajanus cajan* L. Millsp) nodulating rhizobia. *FEMS Microbiol Lett* 2002;216:139–144.
11. Araújo J, Flores-Félix JD, Igual JM, Peix A, González-Andrés F et al. *Bradyrhizobium cajani* sp. nov. isolated from nodules of *Cajanus cajan*. *Int J Syst Evol Microbiol* 2017;67:2236–2241.
12. Jordan DC. Notes: transfer of *Rhizobium japonicum* Buchanan 1980 to *Bradyrhizobium* gen. nov., a genus of slow-growing, root nodule bacteria from leguminous plants. *Int J Syst Bacteriol* 1982;32:136–139.

13. Stępkowski T, Banasiewicz J, Granada C, Andrews M, Passaglia L. Phylogeny and phylogeography of rhizobial symbionts nodulating legumes of the tribe Genisteae. *Genes* 2018;9:163.
14. Aserse AA, Räsänen LA, Aseffa F, Hailemariam A, Lindström K. Phylogenetically diverse groups of *Bradyrhizobium* isolated from nodules of *Crotalaria* spp., *Indigofera* spp., *Erythrina brucei* and *Glycine max* growing in Ethiopia. *Mol Phylogenet Evol* 2012;65:595–609.
15. Avontuur JR, Palmer M, Beukes CW, Chan WY, Coetzee MPA et al. Genome-informed *Bradyrhizobium* taxonomy: where to from here? *Syst Appl Microbiol* 2019.
16. Wang R, Chang YL, Zheng WT, Zhang D, Zhang XX et al. *Bradyrhizobium arachidis* sp. nov., isolated from effective nodules *Arachis hypogaea* grown in China. *Syst Appl Microbiol* 2013;36:101–105.
17. Rivas R, Willems A, Palomo JL, Garcíá-Benavides P, Mateos PF et al. *Bradyrhizobium betae* sp. nov., isolated from roots of *Beta vulgaris* affected by tumour-like deformations. *Int J Syst Evol Microbiol* 2004;54:1271–1275.
18. Vinuesa P, León-Barrios M, Silva C, Willems A, Jarabo-Lorenzo A et al. *Bradyrhizobium canariense* sp. nov., an acid-tolerant endosymbiont that nodulates endemic genistoid legumes (Papilionoideae: Genisteae) from the Canary Islands, along with *Bradyrhizobium japonicum* bv. *genistearum*, *Bradyrhizobium* genospecies alpha and *Bradyrhizobium* genospecies beta. *Int J Syst Evol Microbiol* 2005;55:569–575.
19. Islam MS, Kawasaki H, Muramatsu Y, Nakagawa Y, Seki T. *Bradyrhizobium iriomotense* sp. nov., isolated from a tumor-like root of the legume *Entada koshunensis* from Iriomote Island in Japan. *Biosci Biotech Biochem* 2008;72(6):1416–1429.
20. Kaneko T, Maita H, Hirakawa H, Uchiike N, Minamisawa K et al. Complete genome sequence of the soybean symbiont *Bradyrhizobium japonicum* strain USDA6T. *Genes* 2011;2:763–787.
21. LM X, Ge C, Cui Z, Li J, Fan H. *Bradyrhizobium liaoningense* sp. nov., isolated from the root nodules of soybeans. *Int J Syst Bacteriol* 1995;45:706–711.
22. XM Y, Cloutier S, Tambong JT, Bromfield ESP. *Bradyrhizobium ottawaense* sp. nov., a symbiotic nitrogen fixing bacterium from root nodules of soybeans in Canada. *Int J Syst Evol Microbiol* 2014;64:3202–3207.
23. Grönemeyer JL, Reinhold-Hurek B. Diversity of bradyrhizobia in subsahara Africa: a rich resource. *Front Microbiol* 2018;9.
24. Durán D, Rey L, Mayo J, Zúñiga-Dávila D, Imperial J et al. *Bradyrhizobium paxllaeri* sp. nov. and *Bradyrhizobium icense* sp. nov., nitrogen-fixing rhizobial symbionts of Lima bean (*Phaseolus lunatus* L.) in Peru. *Int J Syst Evol Microbiol* 2014;64:2072–2078.
25. Michel DC, Passos SR, Simões-Araujo JL, Baraúna AC, da Silva K et al. *Bradyrhizobium centrolobii* and *Bradyrhizobium macuxiense* sp. nov. isolated from *Centrolobium paraense* grown in soil of Amazonia, Brazil. *Arch Microbiol* 2017;199:657–664.
26. Guerrouj K, Ruíz-Díez B, Chahboune R, Ramírez-Bahena M-H, Abdelmoumen H et al. Definition of a novel symbiovar (sv. *retamae*) within *Bradyrhizobium retamae* sp. nov., nodulating *Retama sphaerocarpa* and *Retama monosperma*. *Syst Appl Microbiol* 2013;36:218–223.
27. Grönemeyer JL, Kulkarni A, Berkelmann D, Hurek T, Reinhold-Hurek B. Rhizobia Indigenous to the Okavango region in sub-Saharan Africa: diversity, adaptations, and host specificity. *Appl Environ Microbiol* 2014;80:7244–7257.
28. Ndungu SM, Messmer MM, Ziegler D, Gamper HA, Mészáros Éva et al. Cowpea (*Vigna unguiculata* L. Walp.) hosts several widespread bradyrhizobial root nodule symbionts across contrasting agro-ecological production areas in Kenya. *Agric Ecosyst Environ* 2018;261:161–171.
29. Wade TK, Le Quéré A, Laguerre G, N'Zoué A, Ndione JA et al. Eco-geographical diversity of cowpea bradyrhizobia in Senegal is marked by dominance of two genetic types. *Syst Appl Microbiol* 2014;37:129–139.
30. Fossou RK, Ziegler D, Zézé A, Barja F, Perret X. Two major clades of bradyrhizobia dominate symbiotic interactions with pigeonpea in fields of Côte d'Ivoire. *Front Microbiol* 2016;7.
31. Willems A, Coopman R, Gillis M. Phylogenetic and DNA-DNA hybridization analyses of *Bradyrhizobium* species. *Int J Syst Evol Microbiol* 2001;51:111–117.
32. Rivas R, Martens M, de Lajudie P, Willems A. Multilocus sequence analysis of the genus *Bradyrhizobium*. *Syst Appl Microbiol* 2009;32:101–110.
33. Grönemeyer JL, Bünger W, Reinhold-Hurek B. *Bradyrhizobium namibiense* sp. nov., a symbiotic nitrogen-fixing bacterium from root nodules of *Lablab purpureus*, hyacinth bean, in Namibia. *Int J Syst Evol Microbiol* 2017;67:4884–4891.
34. Helene LCF, Delamuta JRM, Ribeiro RA, Ormeño-Orrillo E, Rogel MA et al. *Bradyrhizobium viridifuturi* sp. nov., encompassing nitrogen-fixing symbionts of legumes used for green manure and environmental services. *Int J Syst Evol Microbiol* 2015;65:4441–4448.
35. Auch AF, von Jan M, Klenk HP, Göker M. Digital DNA-DNA hybridization for microbial species delineation by means of genome-to-genome sequence comparison. *Stand Genomic Sci* 2010;2:117–134.
36. Chun J, Oren A, Ventosa A, Christensen H, Arahall DR et al. Proposed minimal standards for the use of genome data for the taxonomy of prokaryotes. *Int J Syst Evol Microbiol* 2018;68:461–466.
37. Broughton WJ, Wong C-H, Lewin A, Samrey U, Myint H. Identification of *Rhizobium* plasmid sequences involved in recognition of *Psophocarpus*, *Vigna*, and other legumes. *J Cell Biol* 1986;102:1173–1182.
38. Kumar S, Stecher G, Tamura K. MEGA7: molecular evolutionary genetics analysis version 7.0 for bigger datasets. *Mol Biol Evol* 2016;33:1870–1874.
39. Gouy M, Guindon S, Gascuel O. SeaView version 4: a multiplatform graphical user interface for sequence alignment and phylogenetic tree building. *Mol Biol Evol* 2010;27:221–224.
40. Rogers JS, Swofford DL. A fast method for approximating maximum likelihoods of phylogenetic trees from nucleotide sequences. *Syst Biol* 1998;47:77–89.
41. Jourand P, Giraud E, Bena G, Sy A, Willems A et al. *Methylobacterium nodulans* sp. nov., for a group of aerobic, facultatively methylotrophic, legume root-nodule-forming and nitrogen-fixing bacteria. *Int J Syst Evol Microbiol* 2004;54:2269–2273.
42. Schwarz G. Estimating the dimension of a model. *Ann Statist.* 1978;6:461–464.
43. Rashid MH-or, Clercx P, Everall I, Wink M, Willems A et al. Average nucleotide identity of genome sequences supports the description of *Rhizobium lentis* sp. nov., *Rhizobium bangladeshense* sp. nov. and *Rhizobium binae* sp. nov. from lentil (*Lens culinaris*) nodules. *Int J Syst Evol Microbiol* 2015;65:3037–3045.
44. Chevreux B, Wetter T, Suhai S. Genome sequence assembly using trace signals and additional sequence information. *Computer Science and Biology. German Conference on Bioinformatics (CGB)*, 99; 1999.
45. Darling AE, Mau B, Perna NT. progressiveMauve: multiple genome alignment with gene gain, loss and rearrangement. *PLoS One* 2010;5:e11147.
46. Seemann T. Prokka: rapid prokaryotic genome annotation. *Bioinformatics* 2014;30:2068–2069.
47. Richter M, Rosselló-Móra R, Oliver Glöckner F, Peplies J. JSpeciesWS: a web server for prokaryotic species circumscription based on pairwise genome comparison. *Bioinformatics* 2016;32:929–931.
48. Richter M, Rosselló-Móra R. Shifting the genomic gold standard for the prokaryotic species definition. *Proc Natl Acad Sci U S A* 2009;106:19126–19131.
49. Martínez-Hidalgo P, Ramírez-Bahena MH, Flores-Félix JD, Igual JM, Sanjuán J et al. Reclassification of strains MAFF 303099T and R7A into *Mesorhizobium japonicum* sp. nov. *Int J Syst Evol Microbiol* 2016;66:4936–4941.

50. Tighe SW, de Lajudie P, Dipietro K, Lindström K, Nick G et al. Analysis of cellular fatty acids and phenotypic relationships of *Agrobacterium*, *Bradyrhizobium*, *Mesorhizobium*, *Rhizobium* and *Sinorhizobium* species using the sherlock microbial identification system. *Int J Syst Evol Microbiol* 2000;50:787–801.
51. Fumeaux C, Bakkou N, Kopćinska J, Golinowski W, Westenberg DJ et al. Functional analysis of the *nifQdctA1y4vGHIJ* operon of *Sinorhizobium fredii* strain NGR234 using a transposon with a NifA-dependent read-out promoter. *Microbiology* 2011;157:2745–2758.
52. Ramírez-Bahena MH, Peix A, Rivas R, Camacho M, Rodríguez-Navarro DN et al. *Bradyrhizobium pachyrhizi* sp. nov. and *Bradyrhizobium jicamae* sp. nov., isolated from effective nodules of *Pachyrhizus erosus*. *Int J Syst Evol Microbiol* 2009;59:1929–1934.
53. Delamuta JRM, Ribeiro RA, Ormeño-Orrillo E, Parma MM, Melo IS et al. *Bradyrhizobium tropiciagri* sp. nov. and *Bradyrhizobium embrapense* sp. nov., nitrogen-fixing symbionts of tropical forage legumes. *Int J Syst Evol Microbiol* 2015;65:4424–4433.

Five reasons to publish your next article with a Microbiology Society journal

1. The Microbiology Society is a not-for-profit organization.
2. We offer fast and rigorous peer review – average time to first decision is 4–6 weeks.
3. Our journals have a global readership with subscriptions held in research institutions around the world.
4. 80% of our authors rate our submission process as 'excellent' or 'very good'.
5. Your article will be published on an interactive journal platform with advanced metrics.

Find out more and submit your article at microbiologyresearch.org.

Supplementary Materials to

***Bradyrhizobium ivorense* sp. nov. as a potential local bioinoculant for *Cajanus cajan* cultures in Côte d'Ivoire**

by **Romain K. Fossou, Joël F. Pothier, Adolphe Zézé and Xavier Perret***

* Corresponding author: xavier.perret@unige.ch

- Table S1.** Origin of the *C. cajan* nodule isolates proposed as *B. ivorense* sp. nov. strains.
- Table S2.** List of primers and sequences of *C. cajan* nodule isolates used in this study.
- Table S3A.** Names and corresponding GenBank accessions for eight type strains selected to represent the *B. japonicum* super clade.
- Table S3B.** Names and corresponding GenBank accessions for the 21 type strains of the *B. elkanii* supergroup that were used for phylogenetic analyses.
- Table S4.** Levels of similarity between concatenated *dnaK-glnII-gyrB-recA-rpoB* sequences of bradyrhizobia.
- Table S5.** Overview and general characteristics of the CI-1B^T and CI-41S genomes.
- Table S6.** Phenotypic characteristics of *B. ivorense* sp. nov. strains and *B. elkanii* USDA 76^T.
- Table S7.** Symbiotic phenotype of selected *B. ivorense* sp. nov. isolates on diverse legumes.
- Figure S1.** Maximum likelihood phylogram inferred from partial 16S rRNA gene sequences.
- Figure S2.** Maximum likelihood phylogram inferred from partial *dnaK* gene sequences.
- Figure S3.** Maximum likelihood phylogram inferred from partial *glnII* gene sequences.
- Figure S4.** Maximum likelihood phylogram inferred from partial *gyrB* gene sequences.
- Figure S5.** Maximum likelihood phylogram inferred from partial *recA* gene sequences.
- Figure S6.** Maximum likelihood phylogram inferred from partial *rpoB* gene sequences.
- Figure S7.** Maximum likelihood phylogram inferred from concatenated partial *glnII* and *recA* gene sequences
- Figure S8.** Maximum likelihood phylogram inferred from partial *nifH* gene sequences.

Table S1. Origin of the *C. cajan* nodule isolates proposed as *B. ivorensis* sp. nov. strains.

	Strain	Plant #	Field # (GPS coordinates)	Locality
1.	<u>CI-1B^T</u> *	1	1 (N 7°17'45" - W 5°49'00")	Kossou-Bouafla
	<u>CI-4A2</u>	4		
	<u>CI-4A3</u>			
	<u>CI-4C</u>			
5.	<u>CI-4D</u>			
	<u>CI-14A</u>	14	3 (N 6°51'19" - W 5°14'38")	Yamoussoukro
	CI-14B	15		
	<u>CI-15A</u>			
	CI-15D			
10.	<u>CI-18C</u>	18	4 (N 6°51'02" - W 5°13'31")	Yamoussoukro
	CI-19A1	19		
	<u>CI-19D</u>			
	CI-19E			
	<u>CI-33F</u>	33	5 (N 7°55'28" - W 2°57'45")	Bondoukou
15.	CI-33K	35		
	<u>CI-35B</u>			
	CI-41B	41	6 (N 7°56'50" - W 2°56'26")	Bondoukou
	CI-41L			
19.	<u>CI-41S</u> *			

Legend to Table S1. Nodule isolates that were sequenced for multilocus sequence analyses (MLSA) are shown in bold and those for which genome data was collected are marked by an asterisk. Strains that are underlined were tested for nodulation and symbiotic nitrogen-fixation on *C. cajan* cvs. ILRI 16555 and "Light Brown". Strains in bold were also inoculated onto *Glycine max* cv. Davis, *Macroptilium atropurpureum* cv. Siratro, *Leucaena leucocephala*, *Tephrosia vogelii*, *Vigna radiata* cv. King and *Vigna unguiculata* cv. Red Caloona, and the phenotypes on these host plants can be found in Table S7.

Table S2. List of primers and sequences of *C. cajan* nodule isolates used in this study.

Primer	5' to 3' sequence	Size (bases)	Amplicon (bp)	Reference
dnaK-For	GGTGACCTTCGACATCGACG	20		this work
dnaK-Rev	CGGTGAACTCCGCGTCGAC	19	461	this work
glnII-For1	TGACCAAGTACAAGCTCGAGT	21		this work
glnII-Rev1	GAGAAGTTGGCGTGCATGCC	20	700	this work
gyrB-For1*	TTCGACCAGAACTCCTACAAGG	22		this work
gyrB-Rev1*	AGCTTGTCCTTGGTCTGCG	19	710	this work
recA-For	CAAGGGCTCGGTGATGAAGC	20		this work
recA-Rev	CGATGCGGCGGATGTCGAG	19	623	this work
rpoB-For	ACGGCACCGAGCGCGTCAT	19		this work
rpoB-Rev	GTCGTCGATCTCGCCCTTGC	20	923	this work

Strain	Gene	Size (bp)	Accession	Reference
CI-1B	16S-ITS-23S	2540	KX396570	Fossou et al. 2016
	<i>dnaK</i>	422	MK376326	this work
	<i>glnII</i>	659	MH756157	this work
	<i>gyrB</i>	669	MH756161	this work
	<i>recA</i>	584	MK376330	this work
	<i>rpoB</i>	923	KX388393	Fossou et al. 2016
CI-14A	16S-ITS-23S	2540	KX396573	Fossou et al. 2016
	<i>dnaK</i>	422	MK376327	this work
	<i>glnII</i>	659	MH756158	this work
	<i>gyrB</i>	669	MH756162	this work
	<i>recA</i>	584	MK376331	this work
	<i>rpoB</i>	884	MK376334	this work
CI-19D	16S-ITS-23S	2539	KX396575	Fossou et al. 2016
	<i>dnaK</i>	422	MK376328	this work
	<i>glnII</i>	659	MH756159	this work
	<i>gyrB</i>	669	MH756163	this work
	<i>recA</i>	584	MK376332	this work
	<i>rpoB</i>	884	MK376335	this work
CI-41S	16S-ITS-23S	2540	KX396584	Fossou et al. 2016
	<i>dnaK</i>	422	MK376329	this work
	<i>glnII</i>	659	MH756160	this work
	<i>gyrB</i>	669	MH756164	this work
	<i>recA</i>	584	MK376333	this work
	<i>rpoB</i>	884	MK376336	this work

Legend to Table S2. *GyrB-For1 and GyrB-Rev1 were derived from gyrB343F and gyrB1043R proposed by Martens et al. (2008).

Table S3A. List of the eight type strains and corresponding GenBank accessions used in this study as data for members of the *Bradyrhizobium japonicum* supergroup. The underlined accession includes one ambiguous (N) position.

	Type strain	Type strain genome data	GenBank accession for corresponding gene					
			16S rRNA	<i>dnaK</i>	<i>glnI</i>	<i>gyrB</i>	<i>recA</i>	<i>rpoB</i>
<i>B. japonicum</i> super clade	<i>B. arachidis</i> CCBAU 051107 ^T	NZ_FPBAQ01000000	HM107167	JX437668	HM107251	JX437675	HM107233	JX437682
	<i>B. betae</i> LMG 21987 ^T	no genome available	<u>AY372184</u>	FM253303	AB353733	AB353735	AB353734	FM253260
	<i>B. canariense</i> BTA-1 ^T	no genome available	AJ558025	AY923047	AY386765	FM253220	AY591553	FM253263
	<i>B. diazoefficiens</i> USDA 110 ^T	NC_004463	gene sequences derived from archived genome data					
	<i>B. iriomotense</i> EK05 ^T	no genome available	AB300992	JF308944	AB300995	AB300997	AB300996	HQ587646
	<i>B. japonicum</i> USDA 6 ^T	NC_017249	gene sequences derived from archived genome data					
	<i>B. liaoningense</i> USDA 3622 ^T	no genome available	AF208513	FM253309	AY386775	FM253223	AY591564	EF190181
	<i>B. ottawense</i> OO99 ^T	CP029425	JN186270	JF308816	HQ587750	HQ873179	HQ587287	HQ587518

Table S3B. Type strains of the *B. elkanii* supergroup and corresponding sequences selected for phylogenetic analyses. Accessions that differ from genome data are shown in bold and those with ambiguous nucleotides (e.g. N, R or Y) are underlined. Note that *recA* of *B. ferriligni* CCBAU 51502^T (KJ818112) was identical to *recA* of *B. elkanii* CCBAU 05737 at both, genomic (NZ_AJPV00000000) and single gene accessions (HM057521).

	Type strain	Type strain genome data	GenBank accession for corresponding gene					
			16S rRNA	<i>dnaK</i>	<i>glnII</i>	<i>gyrB</i>	<i>recA</i>	<i>rpoB</i>
<i>B. elkanii</i> super clade	<i>B. algeriense</i> RST89 ^T	NZ_PYCM01000000	FJ546419	n.a.	FJ264924	n.a.	FJ264927	n.a.
	<i>B. brasiliense</i> UFLA03-321 ^T	NZ_MPVQ01000000	KF311068	KF452791	n.a.	KF452827	KT793142	KF452879
	<i>B. centrolobii</i> BR 10245 ^T	NZ_LUUB01000000	KF927049	KX527928	KX527991	n.a.	KX527954	KF983827
	<i>B. elkanii</i> USDA 76 ^T	NZ_ARAG00000000	HQ233240	AM168363	AY599117	AB070584	AY591568	LC167350
	<i>B. embrapense</i> SEMIA 6208 ^T	NZ_LFIP00000000	AY904773	KP234519	GQ160500	<u>HQ634891</u>	<u>HQ634899</u>	HQ634910
	<i>B. erythrophlei</i> CCBAU 53325 ^T	no genome available	KF114645	MG811656	KF114693	KF114717	KF114669	MG811654
	<i>B. ferriligni</i> CCBAU 51502 ^T	no genome available	KX683400	MG811657	KJ818099	KJ818102	KJ818112	MG811655
	<i>B. icense</i> LMTR 13 ^T	CP016428	KF896156	KF896182	KF896175	KF896201	JX943615	n.a.
	<i>B. jicamae</i> PAC68 ^T	NZ_LLXZ01000000	AY624134	JN207408	FJ428204	HQ873309	HM590776	HQ587647
	<i>B. lablabi</i> CCBAU 23086 ^T	NZ_LLYB01000000	GU433448	KF962687	GU433498	JX437670	GU433522	JX437677
	<i>B. macuxiense</i> BR 10303 ^T	NZ_LNCU01000000	KX527919	KX527932	KX527995	KX528008	KX527958	KX527969
	<i>B. mercantei</i> SEMIA 6399 ^T	NZ_MKFI01000000	FJ025102	KX690617	KX690621	KX690623	KX690615	n.a.
	<i>B. namibiense</i> 5-10 ^T	no genome available	KX661401	KP402058	KM378440	KX661393	KM378377	KM378306
	<i>B. neotropicae</i> BR 10247 ^T	NZ_LSEF01000000	KF927051	KJ661693	KJ661700	KJ661707	KJ661714	KF983829
	<i>B. pachyrhizi</i> PAC48 ^T	NZ_LFIQ01000000	<u>AY624135</u>	JN207406	<u>FJ428201</u>	KF532651	HM047130	LM994172
	<i>B. paxllaeri</i> LMTR 21 ^T	NZ_MAXB01000000	AY923031	AY923038	KF896169	KF896195	JX943617	KP308154
	<i>B. retamae</i> Ro19 ^T	NZ_LLYA00000000	KC247085	LM994150	KC247108	KF962698	KC247094	LM994174
	<i>B. ripae</i> WR4 ^T	no genome available	MF593081	MF593102	MF593086	MF593094	MF593090	MF593098
	<i>B. tropiciagri</i> SEMIA 6148 ^T	NZ_LFLZ01000000	AY904753	FJ391008	FJ391048	<u>HQ634890</u>	FJ391168	HQ634909
	<i>B. valentinum</i> LmjM3 ^T	NZ_LLXX01000000	JX514883	n.a.	JX518575	n.a.	JX518589	n.a.
<i>B. viridifuturi</i> SEMIA 690 ^T	NZ_LGTB01000000	FJ025107	KR149128	KR149131	KR149134	KR149140	KU724169	

Table S4. Similarity levels between concatenated *dnaK-glnII-gyrB-recA-rpoB* (2,560 bp) sequences of bradyrhizobia. Strains were ordered by highest similarity to *B. ivorense* sp. nov. strains CI-1B^T and CI-41S, except for *B. centrolobii* BR 10245^T (#22) and *B. neotropicale* BR 10247^T (#23) that better matched sequences of the *B. japonicum* super-clade representative strain USDA 6^T (#24) shaded in light grey. DNA sequences were from type strains *B. algeriense* RST89^T (#18), *B. brasilense* UFLA03-321^T (#7), *B. elkanii* USDA 76^T (#5), *B. embrapense* SEMIA 6208^T (#9), *B. erythrophlei* CCBAU 53325^T (#13), *B. ferriligni* CCBAU 51502^T (#12), *B. icense* LMTR 13^T (#17), *B. jicamae* PAC68^T (#16), *B. lablabi* CCBAU 23086^T (#14), *B. macuxiense* BR 10303^T (#11), *B. mercantei* SEMIA 6399^T (#10), *B. namibiense* 5-10^T (#19), *B. pachyrhizi* PAC48^T (#6), *B. paxllaeri* LMTR 21^T (#15), *B. retamae* Ro19^T (#20), *B. ripae* WR4^T (#4), *B. tropiciagri* SEMIA 6148^T (#3), *B. valentinum* LmjM3^T (#21) and *B. viridifuturi* SEMIA 690^T (#8). Values above the 97% threshold proposed by Durán et al. (2014) are underlined. Levels of the highest similarity to CI-1B^T and CI-41S are in bold.

	Strain	1	2	3	4	5	6	7	8	9	10	11	12	13	14	15	16	17	18	19	20	21	22	23
1	CI-1B ^T	100			<i>B. ripae</i>	<i>B. elkanii</i>	<i>B. pachyrhizi</i>	<i>B. brasilense</i>	<i>B. viridifuturi</i>	<i>B. embrapense</i>	<i>B. mercantei</i>	<i>B. macuxiense</i>	<i>B. ferriligni</i>	<i>B. erythrophlei</i>	<i>B. lablabi</i>	<i>B. paxllaeri</i>	<i>B. jicamae</i>	<i>B. icense</i>	<i>B. algeriense</i>	<i>B. namibiense</i>	<i>B. retamae</i>	<i>B. valentinum</i>	<i>B. centrolobii</i>	<i>B. neotropicale</i>
2	CI-41S	98.4	100																					
3	<i>B. tropiciagri</i>	95.2	95.3	100																				
4	<i>B. ripae</i>	95.1	95.1	96.6																				
5	<i>B. elkanii</i>	95.1	95.0	96.6	96.7	100																		
6	<i>B. pachyrhizi</i>	95.1	94.9	96.8	96.6	<u>97.8</u>	100																	
7	<i>B. brasilense</i>	95.0	95.1	96.8	96.5	<u>97.9</u>	<u>99.1</u>	100																
8	<i>B. viridifuturi</i>	94.9	94.8	<u>97.2</u>	96.2	96.5	96.5	96.5	100															
9	<i>B. embrapense</i>	94.5	94.5	96.4	95.6	96.5	96.2	96.1	96.2	100														
10	<i>B. mercantei</i>	94.5	94.3	96.7	96.1	96.3	96.3	96.3	96.7	95.5	100													
11	<i>B. macuxiense</i>	94.4	94.6	94.8	94.3	95.6	95.3	95.2	94.6	94.6	94.6	100												
12	<i>B. ferriligni</i>	93.8	93.9	96.2	95.7	96.9	96.9	<u>97.1</u>	95.9	95.6	95.8	94.0	100											
13	<i>B. erythrophlei</i>	93.7	93.9	93.9	93.6	94.1	93.7	93.7	93.9	93.8	93.6	94.1	93.0	100										
14	<i>B. lablabi</i>	91.0	91.3	91.1	90.7	91.5	91.3	91.4	91.3	91.1	91.3	91.3	90.4	90.4	100									
15	<i>B. paxllaeri</i>	91.0	91.3	91.1	91.1	91.3	91.1	91.3	91.2	91.1	91.2	91.0	90.7	90.4	<u>97.1</u>	100								
16	<i>B. jicamae</i>	90.7	91.1	91.0	90.6	91.3	91.0	91.2	90.9	90.9	91.0	91.0	90.5	90.4	96.6	<u>97.4</u>	100							
17	<i>B. icense</i>	90.8	91.0	90.9	91.0	91.5	91.2	91.4	91.0	91.2	91.1	90.7	90.8	90.5	94.5	94.3	94.2	100						
18	<i>B. algeriense</i>	90.4	90.2	90.4	90.0	90.2	90.1	90.4	90.0	89.8	90.5	90.5	89.6	90.2	92.4	92.2	92.2	92.2	100					
19	<i>B. namibiense</i>	90.3	90.8	90.6	90.0	91.0	90.4	90.4	90.5	90.6	90.3	90.7	90.1	90.4	92.2	92.5	92.8	92.3	90.0	100				
20	<i>B. retamae</i>	90.1	90.4	90.7	90.4	90.9	90.7	91.1	90.5	90.8	90.7	90.3	90.1	89.8	94.0	93.6	93.7	95.4	91.6	91.0	100			
21	<i>B. valentinum</i>	89.8	89.9	89.9	89.6	90.0	89.5	89.8	89.6	89.7	89.9	90.0	89.5	89.9	91.9	91.8	91.9	92.2	94.8	90.3	91.1	100		
22	<i>B. centrolobii</i>	90.7	90.8	90.5	90.7	91.0	90.7	90.7	90.8	90.6	90.5	91.1	89.8	91.1	90.1	89.9	89.9	89.5	88.9	90.5	88.8	88.8	100	
23	<i>B. neotropicale</i>	90.5	90.9	90.4	90.2	90.3	90.0	90.1	90.1	90.2	89.9	90.6	89.3	90.5	89.7	89.4	89.6	88.9	88.5	90.2	88.2	88.4	95.7	100
24	<i>B. japonicum</i>	90.5	90.7	91.0	90.9	91.0	90.7	90.8	91.0	90.7	90.5	90.9	90.0	90.1	89.8	89.5	89.6	89.4	89.0	89.5	88.9	89.3	93.7	93.6

Table S5. Overview and general characteristics of the CI-1B^T and CI-41S draft genomes.

	CI-1B^T	CI-41S
Genome size (kb)	9,412	8,864
G+C content (mol%)	64.21	64.37
Number of contigs	44	59
Contig N ₅₀	466,280	253,924
Contig L ₅₀	4	11
Raw coverage	114.6 x	35.7 x
Number of predicted genes	8,546	8,123
Number of tRNAs	56	57

Table S6. Phenotypic characteristics of *B. ivorensis* sp. nov. strains and *B. elkanii* USDA 76^T

Characteristic		CI-1B ^T	CI-14A	CI-19D	CI-41S	USDA 76 ^T
Growth in liquid RMS at (°C)	20	+	+	+	+	+
	25	+	+	+	+	+
	27	+	+	+	+	+
	30	+	+	+	+	+
	35	–	–	w	w	+
	40	–	–	–	–	–
Growth in liquid RMS at pH	4 to 5	–	–	–	–	–
	6 to 8	+	+	+	+	+
	9 to 12	–	–	–	–	–
Growth in RMM with 20 (*10) mM	fructose	w	n.t.	n.t.	w	w
	galactose	+	n.t.	n.t.	+	+
	glucose	+	n.t.	n.t.	+	w
	malate*	+	n.t.	n.t.	+	+
	maltose	–	n.t.	n.t.	–	–
	mannose	w	n.t.	n.t.	w	+
	pyruvate	+	n.t.	n.t.	+	+
	succinate*	+	n.t.	n.t.	+	+
	sucrose	–	n.t.	n.t.	–	–
Growth in YM at 27°C with NaCl at	0.04%	+	+	+	+	+
	0.25%	+	+	+	+	+
	0.5%	+	+	–	w	+
	0.75%	–	–	–	–	w
	1.0%	–	–	–	–	–
Growth on RMS plates with (µg per antibiotic disc)	ampicilin (100)	+	+	w	–	–
	chloramphenicol (500)	+	+	+	+	+
	erythromycin (50)	+	+	+	+	+
	gentamycin (50)	+	+	+	+	+
	kanamycin (100)	+	+	+	+	–
	penicillin (10)	+	+	+	+	+
	streptomycin (250)	+	+	+	+	+
	tetracycline (50)	+	+	+	+	+
Reaction of (API 20NE)	fermentation	–	–	–	n.t.	–
	esculin hydrolysis	w	–	–	n.t.	–
	gelatin hydrolysis	–	–	–	n.t.	–
	arginine di-hydrolase	+	+	+	n.t.	+
	indole production	–	–	–	n.t.	–
	NO ₃ ⁻ reduced to NO ₂ ⁻	–	–	–	n.t.	+
	NO ₃ ⁻ reduced to N ₂	–	–	–	n.t.	–
	urease	+	+	+	n.t.	+
	β-galactosidase (PNPG)	–	–	–	n.t.	–
Assimilation of (API 20NE)	adipic acid	+	+	+	n.t.	+
	capric acid	–	–	–	n.t.	–
	D-glucose	+	w	+	n.t.	w
	D-maltose	+	+	+	n.t.	w
	D-mannitol	+	+	+	n.t.	+
	D-mannose	+	+	+	n.t.	+
	L-arabinose	+	w	+	n.t.	w
	malic acid	w	w	w	n.t.	w
	N-acetylglucosamine	+	+	+	n.t.	w
	phenylacetic acid	w	w	w	n.t.	w
	potassium gluconate	+	+	+	n.t.	+
	trisodium citrate	w	w	w	n.t.	w

Legend to Table S6. +, positive for; –, negative for; w, weak for; n.t., not tested. For details on growth and resistance to antibiotics, see main text. All strains were negative for catalase and positive for oxidase reactions.

Table S7. Symbiotic phenotype of selected *B. ivorensis* sp. nov. isolates on diverse legumes.

Inoculant	Host plant						
	Cc (42 dpi)	Gm (49 dpi)	Ma (42 dpi)	LI (98 dpi)	Tv (42 dpi)	Vr (35 dpi)	Vu (35 dpi)
CI-1B ^T	Nod+ / Fix+	Nod+ / Fix-	Nod+ / Fix+	pNod	Nod+ / Fix+	Nod+ / Fix+	Nod+ / Fix+
CI-14A	Nod+ / Fix+	Nod+ / Fix-	Nod+ / Fix+	n.t.	n.t.	Nod+ / Fix+	Nod+ / Fix+
CI-19D	Nod+ / Fix+	Nod+ / Fix-	Nod+ / Fix+	n.t.	n.t.	Nod+ / Fix+	Nod+ / Fix+
CI-41S	Nod+ / Fix+	Nod+ / Fix-	Nod+ / Fix ^{red}	pNod	Nod+ / Fix+	Nod+ / Fix ^{red}	Nod+ / Fix ^{red}
USDA 76 ^T	Nod+ / Fix+	Nod+ / Fix+	Nod+ / Fix+	n.t.	n.t.	Nod± / Fix ^{red}	Nod+ / Fix+
NGR234	Nod+ / Fix+	Nod-	Nod+ / Fix+	Nod+ / Fix+	Nod+ / Fix+	Nod+ / Fix+	Nod+ / Fix+

Legend to Table S7. The following legumes were tested for nodulation: Cc, *Cajanus cajan* cv. ILRI 16555; Gm, *Glycine max* cv. Davis; Ma, *Macroptilium atropurpureum* cv. Siratro; LI, *Leucaena leucocephala*; Tv, *Tephrosia vogelii*; Vr, *Vigna radiata* cv. King; Vu, *Vigna unguiculata* cv. Red Caloona. Nodulation assays were conducted in Magenta jars with two plants per pot, and with a fixed inoculum of 2×10^8 bacteria in 200 μ l of sterile water per seedling. When needed, plants were watered using B&D nitrogen-free solution. Depending on the host, plants were grown for 35 to 98 days post-inoculation (dpi) before being harvested to assess the symbiotic phenotype of inoculated strains. Capacity of isolates to nodulate was scored as Nod+ for those forming nodules on all inoculated roots, Nod± for sporadic nodules formation, and pNod for strains that made only pseudonodules. Symbiotic nitrogen fixation was scored as strains being capable of sustaining harmonious plant growth (Fix+), poor plant development (Fix^{red}) or no growth beyond seed reserves (Fix-). As positive controls for nodulation and symbiotic nitrogen fixation, control plants were inoculated with strains *Bradyrhizobium elkanii* USDA 76^T or *Sinorhizobium fredii* NGR234. Some plant/strain combinations were not tested (n.t.).

Figure S1. Maximum likelihood phylogram inferred from partial 16S rRNA gene sequences.

The unrooted maximum-likelihood phylogram was inferred from partial 16S rDNA sequences of 57 type strains of the *Bradyrhizobium* genus, of *B. ivorense* sp. nov. strains CI-1B^T and CI-41S (shown in bold) and of *Methylobacterium nodulans* strain ORS 2060^T that was used as the outgroup. Sequences were aligned with MAFFT version 7 using Q-INS-i. The T92+G+I model was used with 1,184 positions and 1,000 pseudoreplicates as parameters. Only bootstrap values >70% are shown at branch nodes. Scale bar indicates the number of substitutions per site.

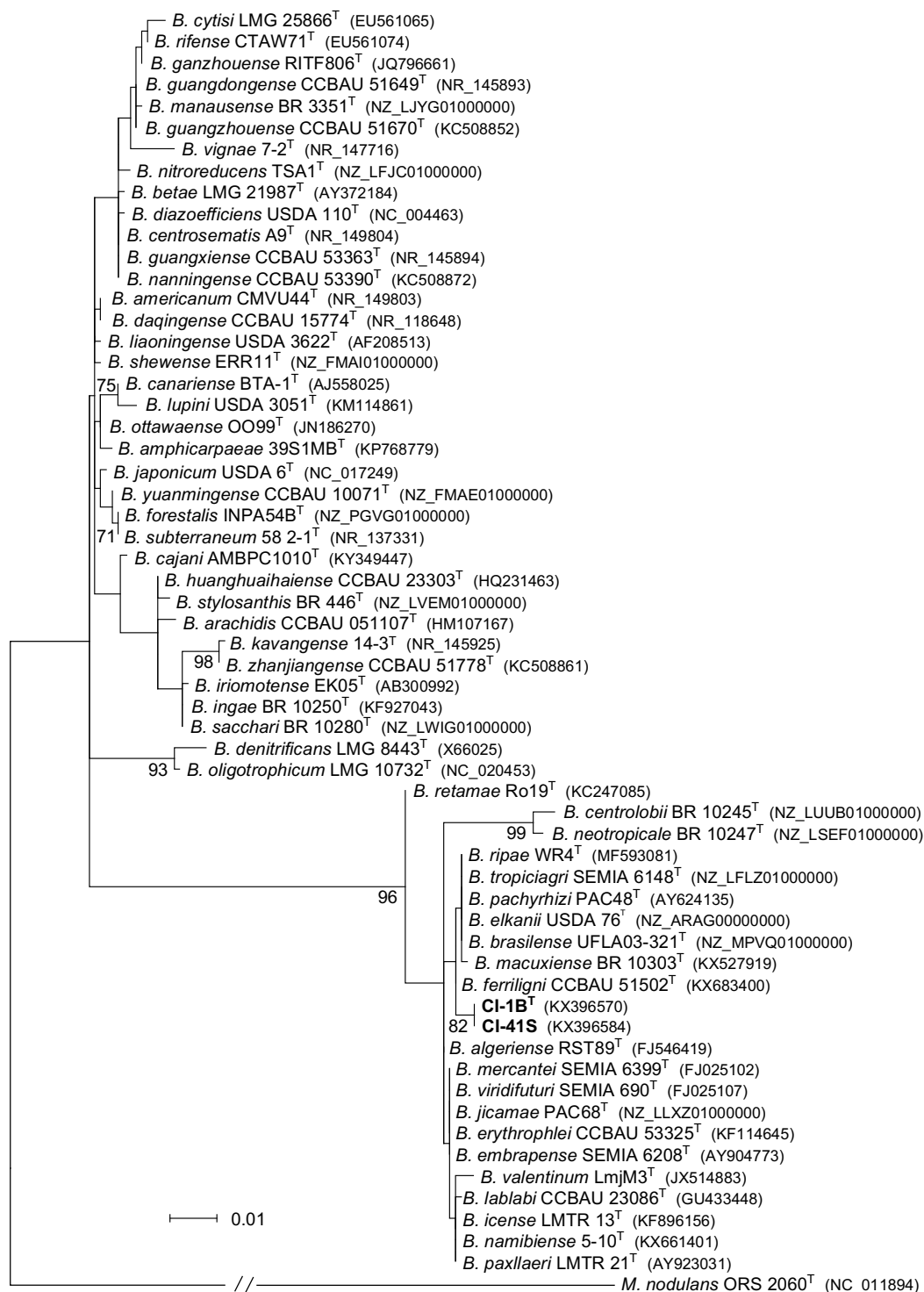


Figure S2. Maximum likelihood phylogram inferred from partial *dnaK* gene sequences.

The unrooted maximum-likelihood phylogram was inferred from 279 bp *dnaK* sequences of type strains of all species included in the *Bradyrhizobium elkanii* supergroup at the time of submission, of a selected number of additional *Bradyrhizobium* species, of *B. ivorense* sp. nov. strains CI-1B^T and CI-41S (shown in bold) and of *Methylobacterium nodulans* strain ORS 2060^T that was used as the outgroup. The TN93+G model was used with 279 positions and 1,000 pseudoreplicates as parameters. Only bootstrap values >70% are shown at branch nodes. Scale bar indicates the number of substitutions per site.

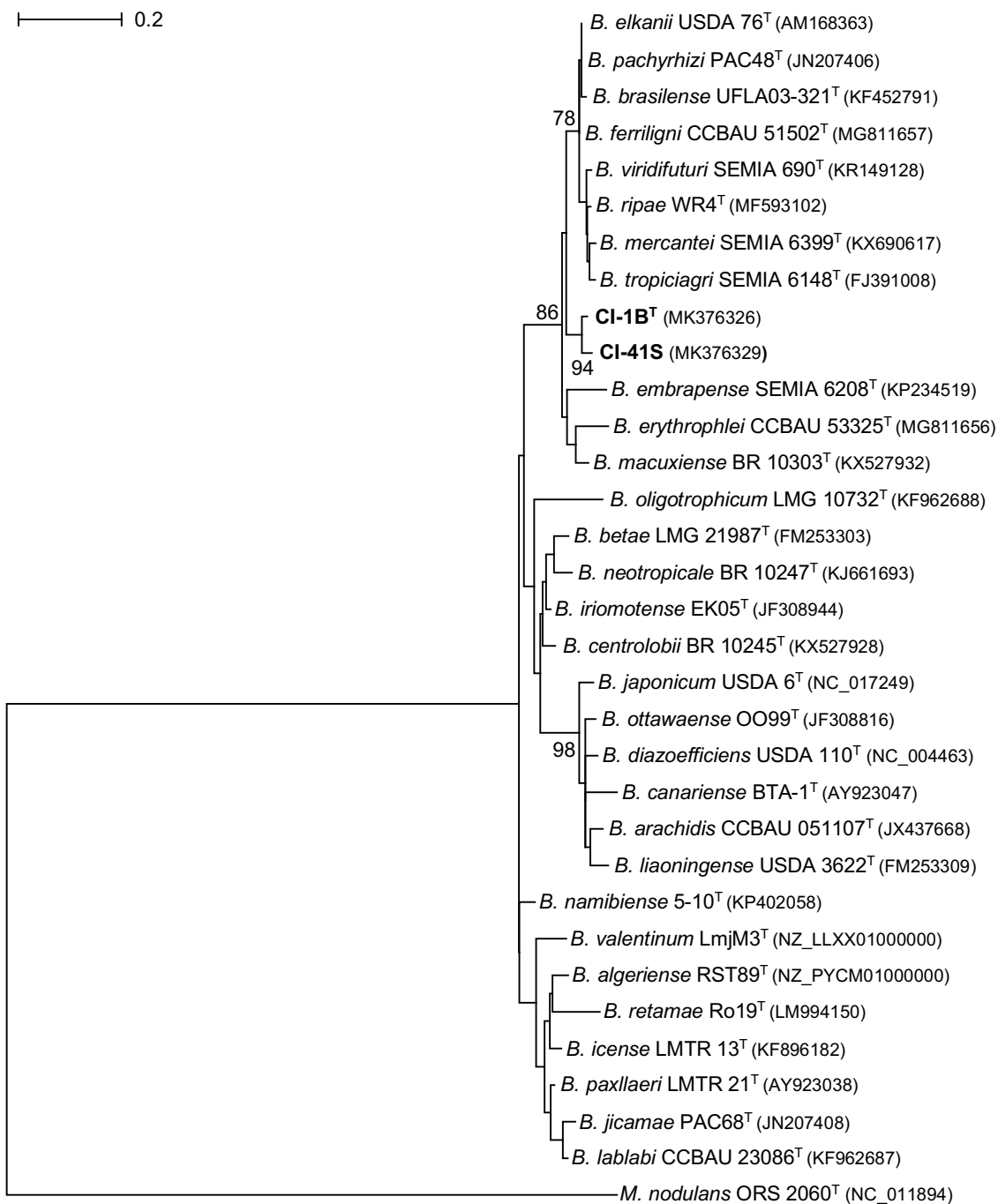


Figure S3. Maximum likelihood phylogram inferred from partial *glnII* gene sequences.

The unrooted maximum-likelihood phylogram was inferred from 540 bp *glnII* sequences of type strains of all species included in the *Bradyrhizobium elkanii* supergroup at the time of submission, of a selected number of additional *Bradyrhizobium* species, of *B. ivorense* sp. nov. strains CI-1B^T and CI-41S (shown in bold) and of *Methylobacterium nodulans* strain ORS 2060^T that was used as the outgroup. The GTR+G+I model was used with 540 positions and 1,000 pseudoreplicates as parameters. Only bootstrap values >70% are shown at branch nodes. Scale bar indicates the number of substitutions per site.

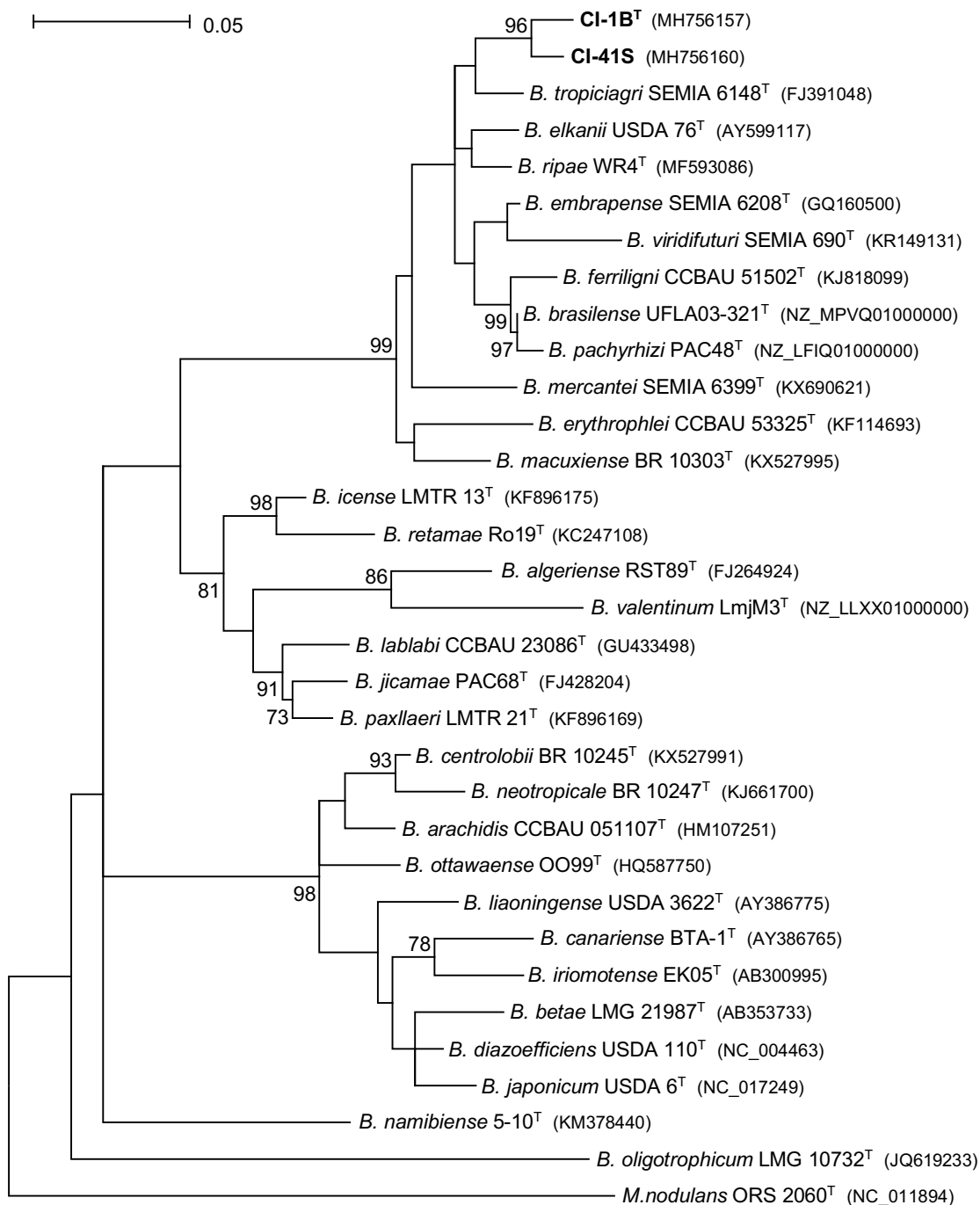


Figure S4. Maximum likelihood phylogram inferred from partial *gyrB* gene sequences.

The unrooted maximum-likelihood phylogram was inferred from 588 bp *gyrB* sequences of type strains of all species included in the *Bradyrhizobium elkanii* supergroup at the time of submission, of a selected number of additional *Bradyrhizobium* species, of *B. ivorense* sp. nov. strains CI-1B^T and CI-41S (shown in bold) and of *Methylobacterium nodulans* strain ORS 2060^T that was used as the outgroup. The T92+G model was used with 594 positions and 1,000 pseudoreplicates as parameters. Only bootstrap values >70% are shown at branch nodes. Scale bar indicates the number of substitutions per site.

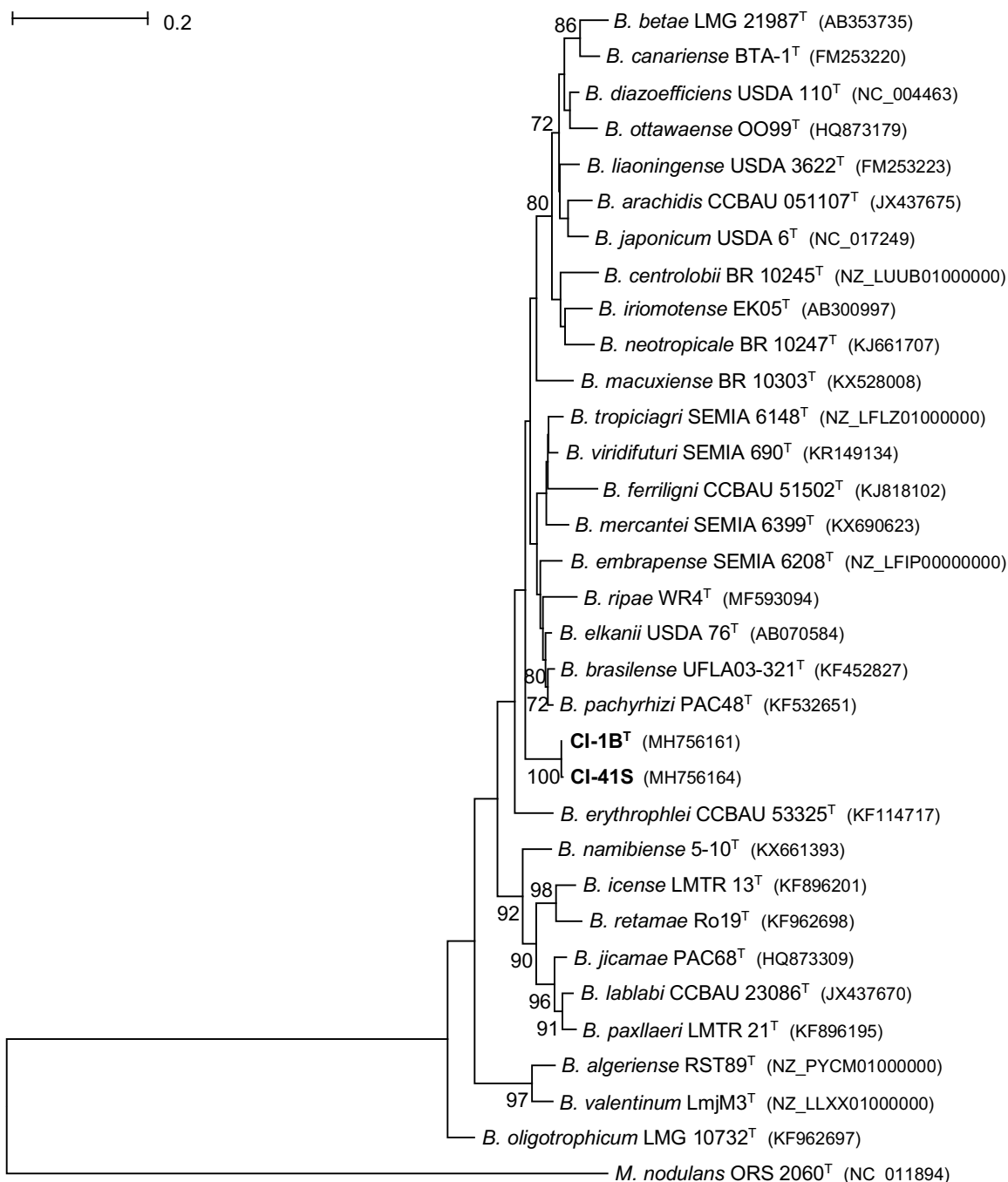


Figure S5. Maximum likelihood phylogram inferred from partial *recA* gene sequences.

The unrooted maximum-likelihood phylogram was inferred from 439 bp *recA* sequences of type strains of all species included in the *Bradyrhizobium elkanii* supergroup at the time of submission, of a selected number of additional *Bradyrhizobium* species, of *B. ivorense* sp. nov. strains CI-1B^T and CI-41S (shown in bold) and of *Methylobacterium nodulans* strain ORS 2060^T that was used as the outgroup. The T92+G model was used with 439 positions and 1,000 pseudoreplicates as parameters. Only bootstrap values >70% are shown at branch nodes. Scale bar indicates the number of substitutions per site.

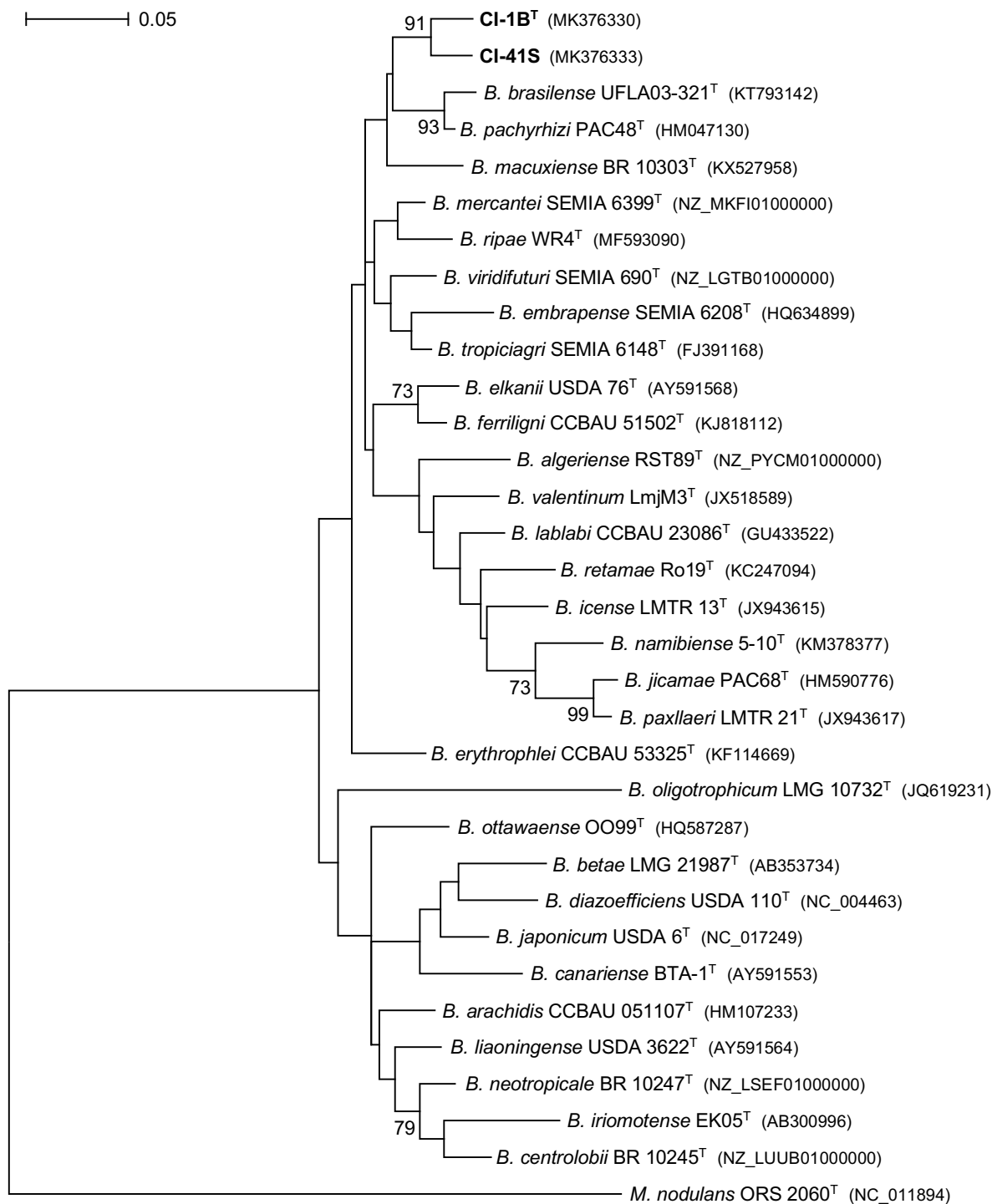


Figure S6. Maximum likelihood phylogram inferred from partial *rpoB* gene sequences.

The unrooted maximum-likelihood phylogram was inferred from 714 bp *rpoB* sequences of type strains of all species included in the *Bradyrhizobium elkanii* supergroup at the time of submission, of a selected number of additional *Bradyrhizobium* species, of *B. ivorense* sp. nov. strains CI-1B^T and CI-41S (shown in bold) and of *Methylobacterium nodulans* strain ORS 2060^T that was used as the outgroup. The GTR+G+I model was used with 714 positions and 1,000 pseudoreplicates as parameters. Only bootstrap values >70% are shown at branch nodes. Scale bar indicates the number of substitutions per site.

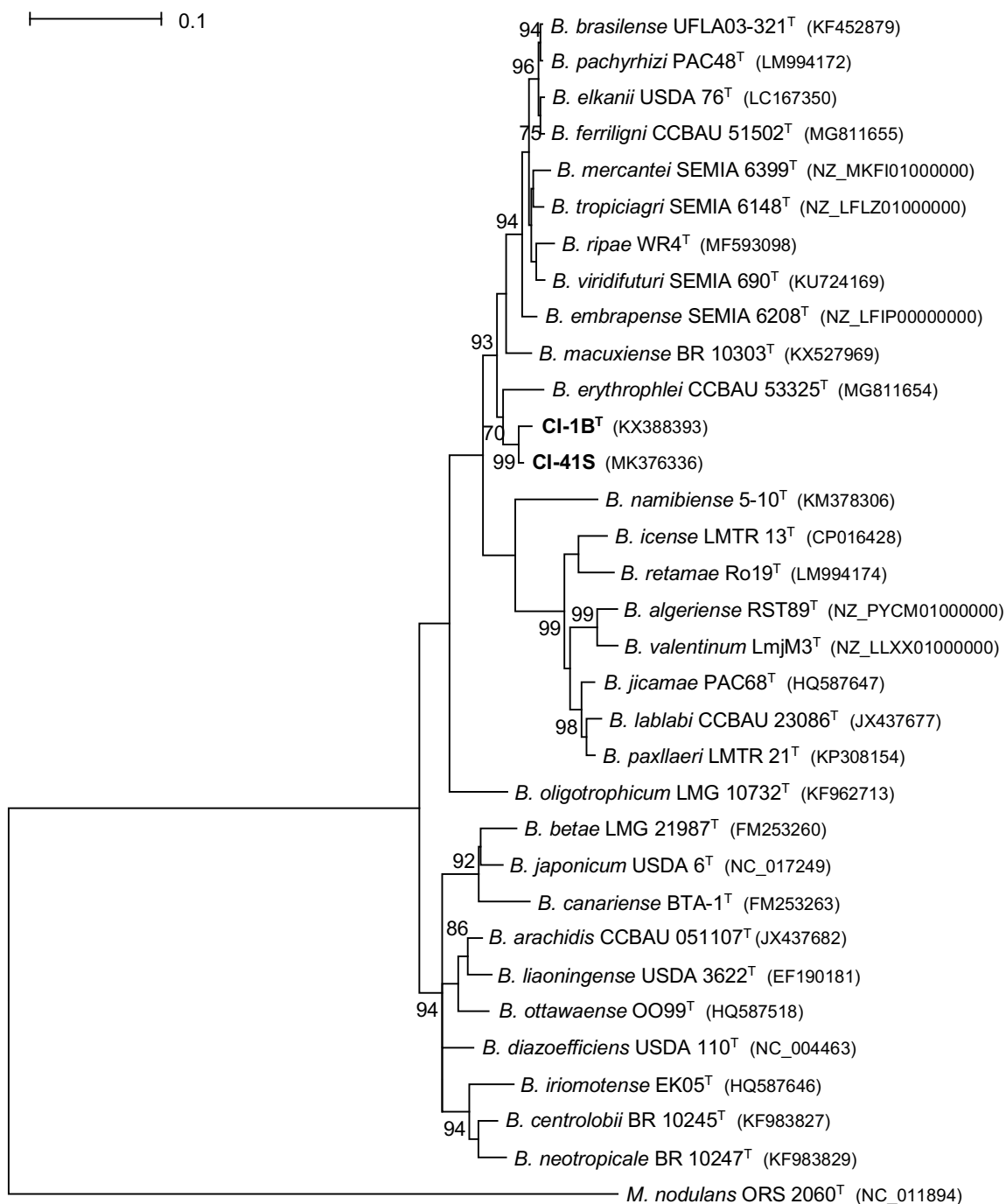


Figure S7. Maximum likelihood phylogram inferred from concatenated *glnII-recA* sequences.

The unrooted maximum-likelihood phylogram was inferred from concatenated partial *glnII* (522 bp) and *recA* (411 bp) sequences of 57 type strains of the *Bradyrhizobium* genus, of *B. ivorense* sp. nov. strains CI-1B^T and CI-41S (shown in bold) and of *Methylobacterium nodulans* strain ORS 2060^T that was used as the outgroup. The GTR+G+I model was used with 933 positions and 1,000 pseudoreplicates as parameters. Only bootstrap values >70% are shown at branch nodes. Scale bar indicates the number of substitutions per site.

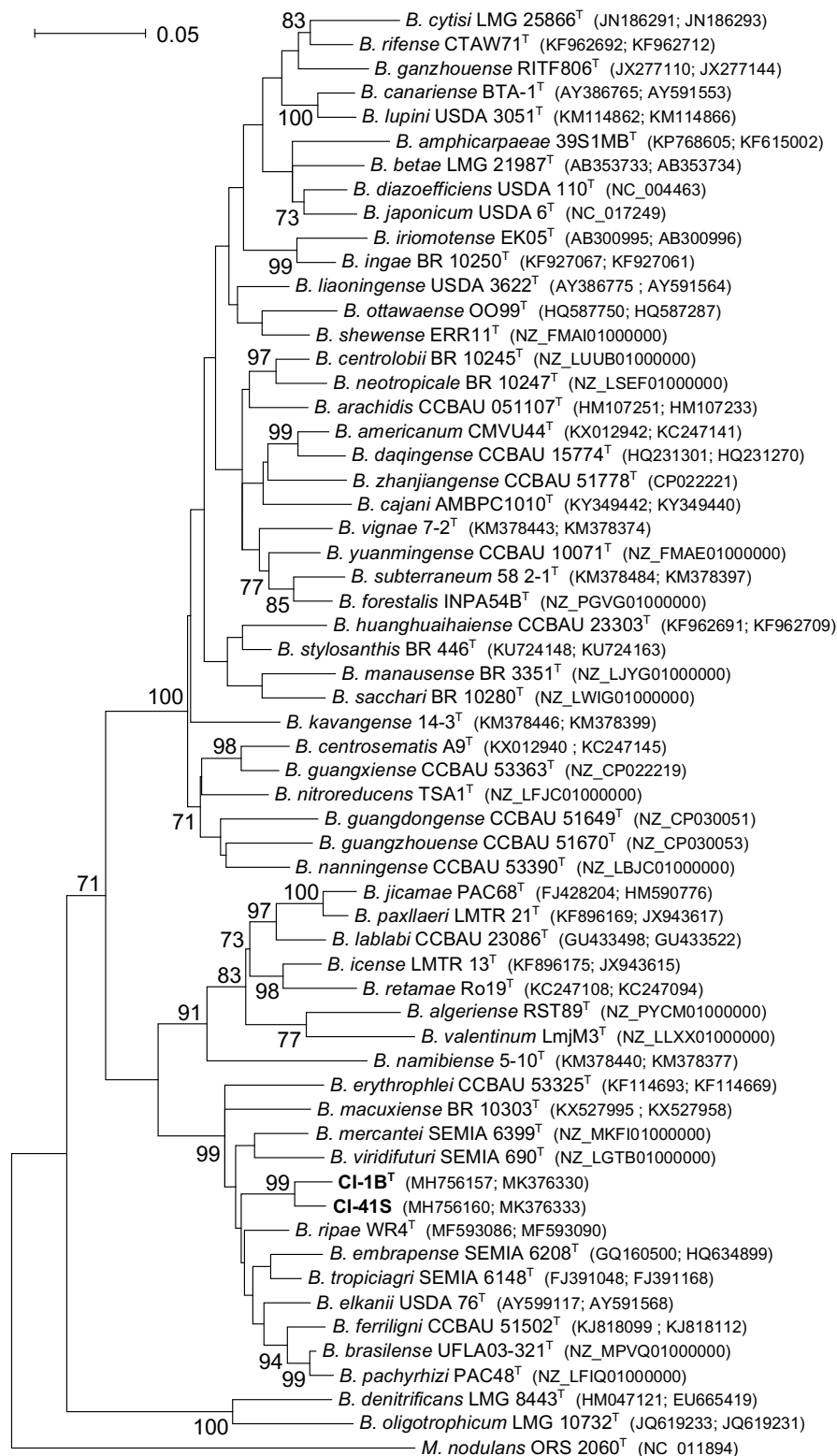


Figure S8. Maximum likelihood phylogram inferred from partial *nifH* gene sequences.

The rooted maximum-likelihood phylogram was inferred from 285 bp *nifH* sequences of type strains of all species included in the *Bradyrhizobium elkanii* supergroup at the time of submission, of a selected number of additional *Bradyrhizobium* species, of *B. ivorense* sp. nov. strains CI-1B^T and CI-41S (shown in bold) and of *Methylobacterium nodulans* strain ORS 2060^T that was used as the outgroup. The T92+G model was used with 285 positions and 1,000 pseudoreplicates as parameters. Only bootstrap values >70% are shown at branch nodes. Scale bar indicates the number of substitutions per site. Genomes of *B. centrolobii* BR 10245^T, *B. neotropicale* BR 10247^T and *B. oligotrophicum* LMG 10732^T were found to code for two divergent copies of *nifH*, both of which were included in this phylogeny. No *nifH* record was found for *B. betae* LMG 21987^T, *B. liaoningense* USDA 3622^T and *B. ripae* WR4^T strains that were included in other gene phylogenies, however.

